JOURNAL OF PETROLOGY | VOLUME 38 | NUMBER 4 | PAGES 495–528 | 1997

Potassic and Sodic Igneous Rocks from Eastern Paraguay: their Origin from the Lithospheric Mantle and Genetic Relationships with the Associated Paraná Flood Tholeiites

P. COMIN-CHIARAMONTI[1]*, A. CUNDARI[2], E. M. PICCIRILLO[3], C. B. GOMES[4], F. CASTORINA[5], P. CENSI[6], A. DE MIN[3], A. MARZOLI[3], S. SPEZIALE[6] AND V. F. VELÁZQUEZ[4]

[1] DIPARTIMENTO DI INGEGNERIA CHIMICA, DELL'AMBIENTE E DELLE MATERIE PRIME, UNIVERSITY OF TRIESTE, PIAZZALE EUROPA 1, I-34127 TRIESTE, ITALY

[2] DIPARTIMENTO DI GEOFISICA E VULCANOLOGIA, 'FEDERICO II' UNIVERSITY, LARGO S. MARCELLINO 10, I-80138 NAPLES, ITALY

[3] DIPARTIMENTO DI SCIENZE DELLA TERRA, UNIVERSITY OF TRIESTE, VIA E. WEISS 8, I-34127 TRIESTE, ITALY

[4] INSTITUTO DE GEOCIÊNCIAS, UNIVERSIDADE DE SÃO PAULO, C.P. 30627, 01051 SÃO PAULO, SP, BRAZIL

[5] DIPARTIMENTO DI SCIENZE DELLA TERRA, 'LA SAPIENZA' UNIVERSITY, PIAZZALE ALDO MORO 5, I-00185, ROME, ITALY

[6] ISTITUTO DI MINERALOGIA, PETROGRAFIA E GEOCHIMICA, UNIVERSITY OF PALERMO, VIA ARCHIRAFI 36, I-90100, PALERMO, ITALY

RECEIVED JUNE 4, 1996 ACCEPTED NOVEMBER 7, 1996

Eastern Paraguay represents the westernmost fringe of Early Cretaceous Paraná flood tholeiites (Serra Geral Formation, SGF). Besides the SGF, eastern Paraguay has been the site of alkaline magmatism since Mesozoic times: (1) Late Permian–Early Triassic sodic intrusions and lavas; (2) Early Cretaceous potassic igneous rocks and very scarce sodic lavas; (3) Late Cretaceous–Oligocene sodic lavas. Two distinct magmatic events are dominant in the Asunción–Sapucai graben (ASU) of eastern Paraguay: (1) widespread potassic magmatism and SGF tholeiites (Early Cretaceous); (2) Asunción sodic magmatism (Late Cretaceous–Oligocene). The potassic rocks form a compositional continuum from moderately to strongly potassic. Two potassic suites are proposed, i.e. basanite to phonolite and alkali basalt to trachyte and their intrusive analogues. The sodic rocks include ankaratrites, nephelinites and phonolites. Two similar but distinct parental magmas have been inferred for the potassic suites, both characterized by strongly fractionated REE and negative 'Ta–Nb–Ti anomalies'. Slight positive Ta and Nb anomalies distinguish the sodic rocks. Sr–Nd isotope data confirm the distinction of the potassic rocks, enriched in radiogenic Sr and low in radiogenic Nd, from the sodic rocks, close to bulk Earth. Crustal contamination does not appear to have been significant in the generation of the investigated rocks, supported by $\delta^{18}O$ data. The source of potassic rocks is constrained by high LILE, LREE, Th, U and K, relative to a primitive mantle composition, and a garnet peridotite is favoured as a possible mantle source for the investigated rocks. The close association of potassic and sodic rock suites in the ASU demands that their parental magmas derived from a heterogeneous subcontinental mantle, variously enriched in incompatible elements. Significant H_2O, CO_2 and F are expected in the mantle source(s) for the occurrence of coeval carbonatites. Any genetic hypothesis based on a 'mantle plume' system is constrained by strong lithospheric mantle characteristics. This does

* Corresponding author. Fax: 0039 40 569 823.

not preclude that thermal perturbations from the asthenosphere may have triggered magmatic activity in the lithospheric mantle. Model ages indicate that two distinct metasomatic events may have occurred during Late and Early–Middle Proterozoic as precursor to the genesis of tholeiitic and alkaline magmatism in the Paraná Basin. These metasomatic processes were chemically distinct, indicated by the strong differences in Ti, LILE and HFSE concentrations found in both alkaline provinces (e.g. potassic rocks from ASU vs Alto Paranáiba Igneous Province) and Paraná tholeiites (low vs high Ti). In general, the relationships between the alkaline rocks from southeastern Brazil, i.e. Alto Paranaíba, Ponta Grossa Arch, Serra do Mar, Lages and the flood basalts of the Paraná Basin, support a common origin in the lithospheric mantle. Sr–Nd isotope and other geochemical data indicate that a significant role was played by a mantle component depleted in incompatible elements and with high Sm/Nd ratio. This component (N-MORB type) would be represented by the depleted portions of a mantle which was variously metasomatized during Proterozoic times. The isotopic and geochemical features of the modern Tristan da Cunha plume are distinctly different from the component depleted in incompatible elements, and its contribution is not apparent in the compositions of the Paraná tholeiites.

KEY WORDS: *Alkaline magmatism; Paraguay; petrogenesis; Sr–Nd isotopes*

INTRODUCTION

Potassic magmatism, *sensu* Foley *et al.* (1987), generally occurs in different tectonic settings. This magmatism is characterized by high concentration of incompatible elements (IE), besides high K, which makes its genesis by partial melting of conventional peridotite mantle sources unlikely (Wyllie, 1987). A 'veined' mantle source enriched by various degrees of mantle metasomatism under variable redox conditions has been proposed by Foley (1988), although the nature of the enriched component(s) has not been uniquely identified, and the role of the tectonic regime and related mantle dynamics at the time of potassic magma genesis remains only partly understood.

For example, mafic potassic rocks from the Alto Paranaíba Province of SE Brazil, widespread in an area of crustal thinning (Santero *et al.*, 1988), have been related to a mantle plume, which made contact with and melted the most fusible parts of lithospheric mantle at the margins of the São Francisco craton during Late Cretaceous times (Gibson *et al.*, 1995*b*). However, mafic potassic rocks are not exclusive to cratonic or mobile belt settings (e.g. Bergman, 1987; Foley *et al.*, 1987) nor are they confined to regions where the lithosphere is especially thin, e.g. New South Wales (Ewart *et al.*, 1988; Ewart, 1989).

This paper seeks to evaluate new petrological information on the alkaline magmatism of the western margin of the Paraná Basin, where a variety of potassic rocks are associated in time and space with sodic rocks and carbonatites. The investigated rocks occur in eastern Paraguay and span the Mesozoic to Eocene–Oligocene times. Therefore, they are germane to the magmatic and tectonic evolution of the Paraná Basin generally and to the petrogenesis of alkaline rocks from a continental setting in particular. It will be demonstrated that these rocks are closely related to magmatic and tectonic events responsible for the formation of the Paraná tholeiitic flood basalts. Implications and constraints for the origin and evolution of the magmatic activity in and around the Paraná Basin are discussed, also in the light of recent data on the potassic magmatism from Alto Paranaíba Igneous Province (SE Brazil; Gibson *et al.*, 1995*b*).

GEOLOGICAL SETTING

Eastern Paraguay lies along the former western margin of Gondwana, in an intercratonic region which includes the western side of the Paraná Basin of Brazil, bounded by an anticlinal structure established since Early Palaeozoic, the Asunción Arch (Fig. 1), which separates the Paraná Basin (east) from the Gran Chaco Basin (west). The basement formations are largely Precambrian to Early Palaeozoic granitic intrusions and high-grade metasedimentary rocks, considered the northernmost occurrence of the Rio de la Plata craton, and the southernmost tip of the Amazon craton (Fulfaro, 1996). Eastern Paraguay was subjected to NE–SW-trending crustal extension during Late Mesozoic, probably related to the western Gondwana break-up and the opening of the South Atlantic. NW–SE fault trends, consistent with the dominant orientation of Mesozoic alkaline and tholeiitic dykes, reflect this type of structure. These are crosscut by NE–SW lineaments apparently related to Precambrian–Cambrian basement structures reactivated and enhanced by Early Cretaceous events (Fulfaro, 1996). The resulting structural pattern controlled the development of the associated grabens as a response to NE–SW-directed extension and continued evolving into Upper Tertiary times. Notable for its high concentration of alkaline rocks is the Asunción–Sapucai graben (ASU), ~200 km long and 25–40 km wide, filled with sediments up to 2·5 km thick (Hegarty *et al.*, 1996).

From the beginning of Mesozoic times, four main magmatic events have occurred in eastern Paraguay. The oldest one (Alto Paraguay Province), is represented by ring complexes of nepheline syenites to alkaline granites and their effusive equivalents, dated at Late Permian–Early Triassic (240–250 Ma; Comin-Chiaramonti & Gomes, 1996). This magmatism is widespread at the southernmost side of the Guaporé Craton. The second event is represented by the flood tholeiites of the Alto Paraná Formation, i.e. Serra Geral Formation (SGF), of Brazil. ^{40}Ar–^{39}Ar dates from SGF flood tholeiites, obtained from specimens distributed over the entire Paraná Basin, yielded a range of 127–137 Ma (Turner *et al.*, 1994). SGF specimens from the SE margin of the Basin gave well-constrained ^{40}Ar–^{39}Ar dates of 133 ± 1 Ma (Renne *et al.*, 1992), 132 ± 1 Ma and 133 ± 3 Ma (Turner *et al.*, 1994). P. R. Renne (personal communication, 1995) reported a ^{40}Ar–^{39}Ar date of 133 ± 1 Ma from one SGF specimen from Foz do Iguaçu, at the Paraguay state border. The third magmatic event, essentially represented by potassic rocks (137–118 Ma), predated the SGF tholeiites in the Rio Apa and Amambay (NE Paraguay) regions, and postdated the same in the ASU. A biotite ^{40}Ar–^{39}Ar date from the Cerro Chararà (i.e. Cerro Santo Tomás, ASU) potassic intrusion in eastern Paraguay gave $126{\cdot}8 \pm 0{\cdot}3$ Ma (Renne *et al.*, 1993). Over 200 alkaline basaltic dykes with dominant NW–SE orientation are associated with alkaline complexes and lava flows in the ASU. Carbonatites occur in the Rio Apa, Amambay and ASU regions (Castorina *et al.*, 1994). Sodic alkaline rocks (120 Ma, K/Ar whole-rock, one sample; J. DeGraff, personal communication, 1995), containing abundant mantle xenoliths, occur as plugs and dykes in the San Juan Bautista region. Finally, the youngest magmatism (70–32 Ma; Comin-Chiaramonti *et al.*, 1991) is represented by ultra-alkaline sodic rocks containing mantle xenoliths (Comin-Chiaramonti *et al.*, 1986), phonolitic plugs and tephritic to phonolitic dykes near Asunción township. The estimated volumes are ~500, 20 000, 1200 and 100 km^3 for the Alto Paraguay Province, SGF, ASU potassic Province and San Juan Bautista Province plus ASU sodic magmatism, respectively.

CLASSIFICATION AND PETROGRAPHY

A total of 527 specimens from the ASU Province, inclusive of dyke rocks, have been investigated in detail, and particulars of field, age, petrography and mineral chemistry have been given by Comin-Chiaramonti & Gomes (1996). Rock nomenclature is after de la Roche (1986).

The fine-grained nature of most ASU rocks prompted the adoption of a chemical classification based on that of LeMaitre (1989). The following subdivisions were adopted, on the basis of our chemical database from Paraguay:

$Na_2O - 2 \geq K_2O$ for sodic compositions (Na);
$1 < K_2O/Na_2O \leq 2$ for potassic compositions (K);
$Na_2O - 2 < K_2O$ and $K_2O/Na_2O \leq 1$ for compositions transitional to K (tK);
$K_2O/Na_2O > 2$ for highly potassic compositions (HK).

Of the analysed ASU specimens, 18% are Na, 57% K, 18% tK and 7% HK types. Their distribution, illustrated in Fig. 2, shows that the variation of the dyke rocks is consistent with that of the associated intrusive and volcanic rocks and, with the possible exception of the ankaratrites–nephelinites, the ASU compositional variation is virtually continuous. K, HK and tK types generally fall in Barton's (1979) 'Roman Region Type' field and in the Foley *et al.* (1987) 'Group III'. Notably, only 7% of the compositions are 'ultrapotassic', namely, $K_2O/Na_2O > 2$, $K_2O > 3$ wt %, $MgO > 3$ wt %. The ASU compositions straddle the alkali basalt to trachyte and the basanite–tephrite to phonolite fields of de la Roche's (1986) diagram (Fig. 2), as well as the corresponding boundary between their TAS analogues (LeBas *et al.*, 1986), i.e. basanite–tephrite to phonolite and trachybasalt to trachyte, respectively. Modal analyses of medium- to coarse-grained potassic intrusives representative of the ASU compositional spectrum, projected into Streckeisen's (1976) QAPF diagram (Fig. 3), suggest two main suites, i.e. basanite to phonolite (B–P) and alkali basalt to trachyte (AB–T) (see Fig. 2).

The sodic rocks

These are mainly represented by ankaratrites + nephelinites (45%), and phonolites (42%).

Ankaratrites and nephelinites contain olivine (Fo_{82-78}), clinopyroxene ($Wo_{47}Fs_{11}$) and magnetite (ulv. 38%) phenocrysts or microphenocrysts in hypocrystalline groundmass composed of 40–49 vol. % salite ($Wo_{50}Fs_{13}$), 7–16 vol. % olivine (Fo_{74-78}) and 4–8 vol. % titanomagnetite (ulv. 43%) + nepheline + apatite ± alkali feldspar ± biotite ± carbonate ± glass. Mantle lherzolite, harzburgite and dunite xenoliths and xenocrystic debris are common and abundant.

Phonolites are typically microphyric to hypocrystalline with alkali feldspar phenocrysts or microphenocrysts (Or_{43-83}), nepheline (Ne_{67-79}), occasionally altered to cancrinite, acmitic clinopyroxene (acmite up to 63 wt %) and ferroedenite–ferropargasite amphibole. Haüyne, mica, haematite and zircon are typical accessory minerals. Analcime occurs as a nepheline pseudomorph. Ti-andradite and sphene occur in some dykes.

The potassic rocks

B–P suite

Theralites, essexitic gabbros, ijolites and essexites are holocrystalline, seriate, with diopsidic pyroxene (Wo_{44-51} Fs_{8-17}), olivine (Fo_{75-82} to Fo_{44-66}), mica (Ti-phlogopite to Ti-biotite), Ti-magnetite, alkali feldspar, nepheline ($Ne_{64-80}Ks_{20-36}$) ± leucite ± amphibole. Leucite pseudomorphed by analcime and plagioclase are common in

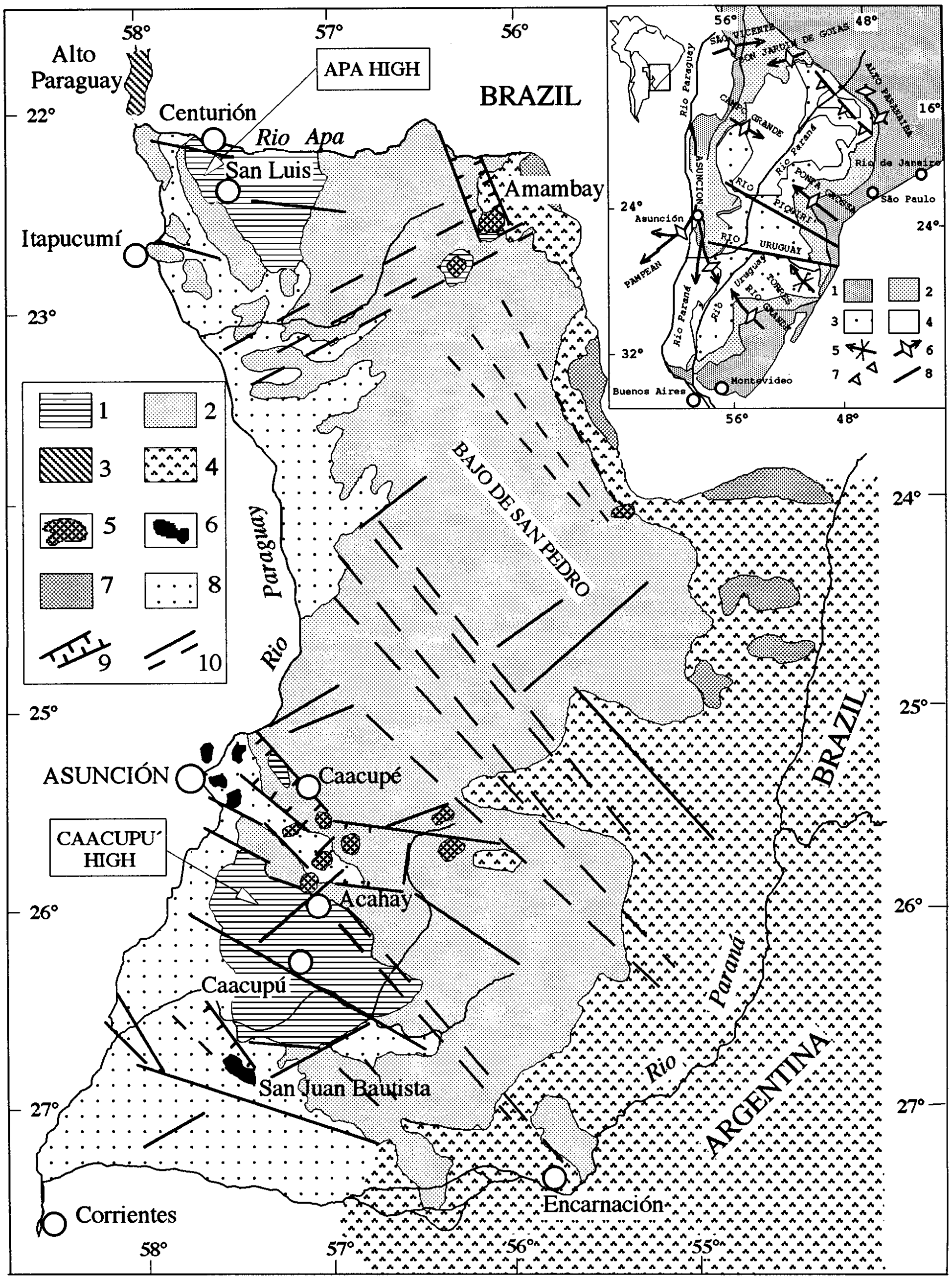

Fig. 1. Generalized geological map of eastern Paraguay. 1, Precambrian–Cambrian crystalline basement: high-grade metasedimentary rocks and granitic intrusions. 2, Cambrian to Triassic–Jurassic: limestones, sandstones, arkoses, conglomerates, siltites, granitic intrusions and quartz–porphyry lava flows. 3, Late Permian–Early Triassic (250–240 Ma); mainly Na syenites and effusive equivalents (Alto Paraguay Province). 4, Early Cretaceous (137–133 Ma) flood tholeiites ('Alto Paraná Formation' corresponding to the Brazilian 'Serra Geral Formation'). 5, Early Cretaceous (137–118 Ma) potassic rocks. 6, Early Cretaceous (~120 Ma) nephelinitic plugs and dykes of San Juan Bautista; Palaeogene (70–32 Ma) nephelinitic and phonolitic lava flows, dykes and necks of Asunción. 7, Upper Cretaceous: aeolian sandstones ('Acaray Formation' corresponding to the bottom of the Brazilian 'Bauru Group'). 8, Tertiary–Quaternary alluvial cover. 9, Graben. 10, Faults. Inset: generalized sketch-map of the Paraná Basin. 1, Pre-Devonian crystalline basement; 2, pre-volcanic sediments (mainly Palaeozoic); 3, basic, intermediate and acid volcanics (Serra Geral Formation); 4, post-volcanic sediments (mainly Upper Cretaceous); 5, syncline; 6, arch; 7, flexure; 8, Rio Piquirí and Rio Uruguay tectonic lineaments.

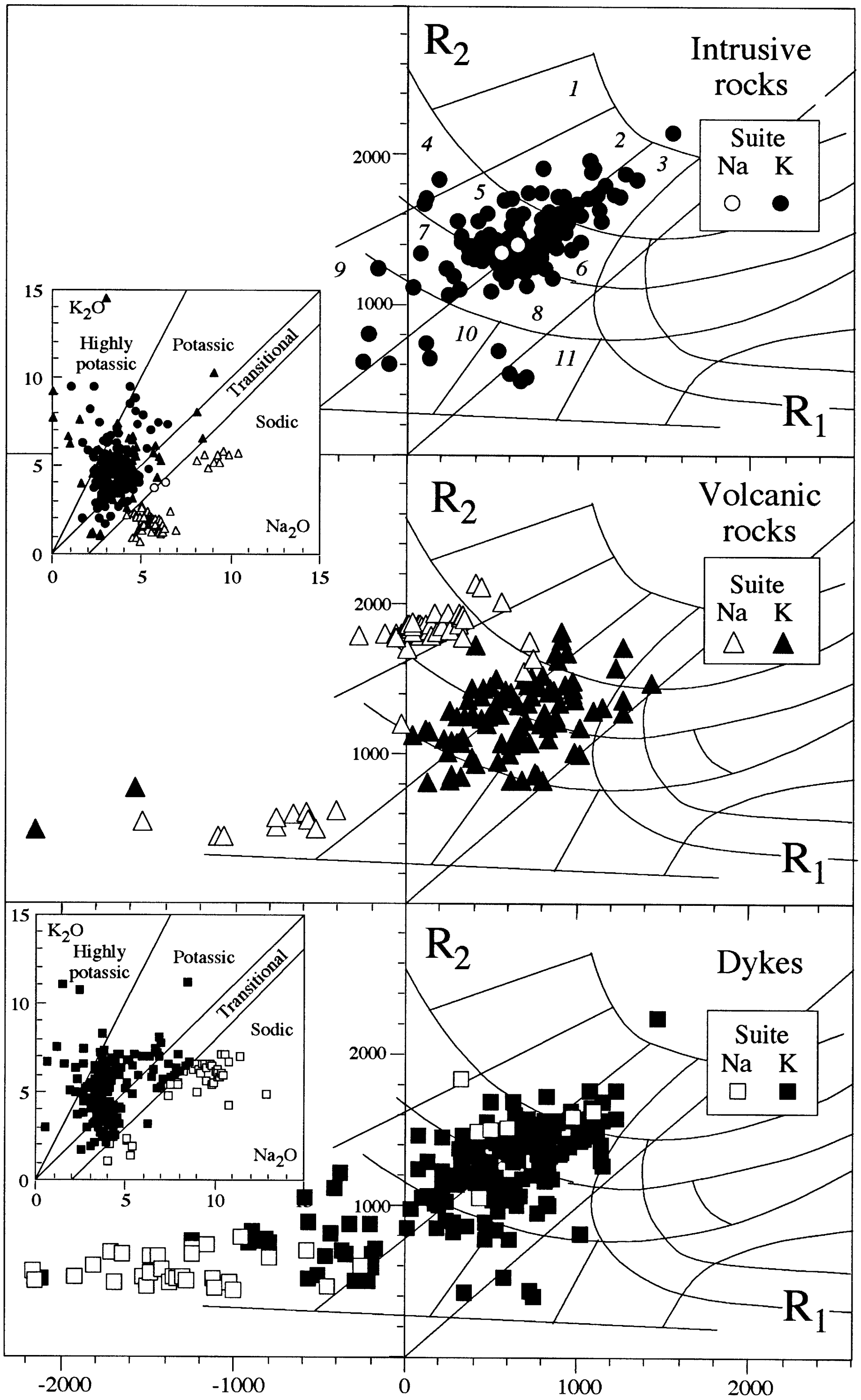

Fig. 2. ASU compositional variation in terms of de la Roche's (1986) diagram; $R_1 = 4Si - 11(Na+K) - 2(Fe+Ti)$, $R_2 = 6Ca + 2Mg + Al$. Data source: Comin-Chiaramonti & Gomes (1996). Numbers correspond to the fields of de la Roche's nomenclature, the intrusive equivalents being given in parentheses: 1, ankaratrite (melteigite); 2, basanite (theralite); 3, alkali basalt (alkali gabbro); 4, nephelinite (ijolite); 5, tephrite (essexitic gabbro); 6, trachybasalt (syenogabbro); 7, phonotephrite (essexite); 8, trachyandesite (nepheline syenodiorite); 9, phonolite (nepheline syenite); 10, trachyphonolite (nepheline syenite); 11, trachyte (syenite). Insets: K_2O vs Na_2O (wt %) diagram for intrusive, effusive and dyke rocks from ASU.

Table 1: Representative whole-rock analyses from Eastern Paraguay

	1	2	3	4	5	6	7	8	9	10	11	12	13	14	15
Locality:	Mbocayaty	Cerro E Santa Elena	Aguapety Portón	Cañada	Aguapety Portón	Cerro San Benito	Cerro Km 23	Sapucai	Cerro San José	Cerro Arrúa-í	Sapucai	Cerro Santo Tomás	Sapucai	Sapucai	Sapucai
Suite:	B–P, HK	B–P, HK	B–P, HK	B–P, K	B–P, K	B–P, K	B–P, tK	B–P, K	B–P, tK	B–P, tK	B–P, HK	B–P, K	B–P, K	B–P, K	B–P, tK
Rock type:	Essexitic gabbro	Essexite	Essexitic gabbro	Ijolite	Theralite	Essexite	Essexite	Phono-tephrite	Phono-tephrite	Phonolite	Phonolite	Basanite	Tephrite	Phono-tephrite	Tephrite
Sample:	51-3152	39-PS530	52-PS264	77-PS245	56-PS268	27-PS535	21-PS539	143-PS31	100-PS233	257-PS201	D110-102	D211-3088	D207-PS111	D151-PS28	D122-PS34
wt %															
SiO_2	48·20	47·36	48·33	44·11	41·96	51·32	50·81	52·88	50·51	53·14	47·05	46·83	48·50	48·78	44·17
TiO_2	1·92	1·66	1·91	2·01	2·94	1·38	1·13	1·40	1·58	1·17	1·90	1·62	1·56	1·59	2·29
Al_2O_3	10·35	14·86	12·92	12·82	10·22	15·13	16·47	17·95	16·98	16·69	15·87	12·46	13·18	17·67	12·78
Fe_2O_3	4·98	1·31	2·56	4·45	6·25	1·99	2·81	3·22	2·48	4·13	4·15	4·48	5·17	3·53	7·05
FeO	5·42	6·96	7·24	5·15	6·40	5·24	4·68	3·55	5·78	2·82	4·43	3·86	4·48	4·98	4·96
MnO	0·20	0·12	0·17	0·19	0·22	0·13	0·16	0·14	0·15	0·15	0·14	0·15	0·14	0·16	0·18
MgO	10·91	6·36	6·62	9·53	12·11	3·83	3·56	2·78	4·20	3·01	3·73	9·78	7·48	4·04	6·96
CaO	7·93	8·80	9·08	10·32	12·48	6·58	7·76	5·54	7·85	5·07	6·73	9·37	8·73	7·34	10·19
Na_2O	2·00	1·08	2·54	3·34	1·63	3·55	4·82	4·54	4·44	5·89	3·66	3·06	2·71	4·02	3·30
K_2O	5·81	9·45	5·81	5·41	2·04	7·09	4·37	5·84	3·89	4·21	8·31	4·04	4·69	5·00	3·26
P_2O_5	0·56	0·20	0·86	0·75	0·86	0·64	0·53	0·50	0·55	0·71	0·67	0·52	0·37	0·59	0·56
LOI	1·61	1·46	1·25	1·23	3·27	2·12	1·83	0·88	1·20	2·51	2·33	3·62	1·99	1·24	3·14
Total	99·89	99·62	99·29	99·31	99·38	99·00	98·93	99·22	99·61	99·50	98·97	99·79	99·00	98·94	98·84
mg-no.	0·70	0·62	0·59	0·68	0·68	0·53	0·51	0·47	0·52	0·54	0·53	0·72	0·63	0·51	0·56

p.p.m.															
La	109	21	83	108	106	114	84	88	69	98	98	88	84	88	106
Ce	196	51	164	204	204	207	153	157	134	179	186	140	140	163	161
Pr		7·0	18·5	23·8				18·4		20·3		15·3	15·3	16·2	19·40
Nd	76·5	44·3	66·3	90·2	93·7	83·6	64·8	62·6	62·7	74·6	63·2	60·6	63·8	55·2	73·40
Sm	11·3	7·9	11·1	13·8	14·4	12·3	10·12	10·05	10·6	12·68	15·9	10·8	12·80	8·9	20·00
Eu	2·88	3·77	3·04	3·67	3·86	3·23	2·76	2·63	3·00	3·46	2·02	2·50	2·38	2·6	3·60
Gd	7·46	5·66	5·81	9·09	9·63	7·88	6·89	6·98	7·92	8·91	5·93	6·40	6·40	6·5	8·40
Tb		0·75		1·11				0·90		1·06	0·59	0·75	0·74	0·90	0·67
Dy	3·42	3·3	3·79	4·70	4·90	3·96	3·60	4·47	3·85	4·88	2·86	4·05	3·25	3·61	3·61
Ho		0·39		1·09				0·79		0·84		0·68	0·64		0·78
Er	1·55	0·67	1·47	1·77	2·08	1·68	1·67	2·06	1·62	2·40	1·59	1·90	1·80	2·20	2·22
Tm		0·05		0·24				0·35		0·29		0·28	0·23		0·34
Yb	1·07	0·27	1·16	1·36	1·46	1·29	1·35	1·93	1·30	1·68	1·59	1·69	2·00	1·30	1·97
Lu	0·20	0·05	0·24	0·24	0·27	0·23	0·26	0·34	0·24	0·31	0·23	0·25	0·20	0·20	0·29
Cr	868	122	241	288	310	70	19	25	57	42	53	395	476	29	190
Ni	297	60	56	109	98	34	20	9	22	25	22	124	88	21	85
Rb	190	337	136	114	69	146	65	128	81	103	260	89	108	105	69
Ba	1469	715	1741	1958	768	1776	1322	1425	1142	1094	1935	1218	1448	1325	1626
Th	11·32	2·2	6·2	6·6	6·83	13·2	13·8	10·9	9·1	24·5	12·7	13·2	11·3	10·6	13·8
U	2·43	0·2	1·9	1·7	1·47	2·5	2·5	25	2·4	5·8	3·5	2·6	2·1	2·3	2·7
Ta	3·5	1·8	2·4	3·1	2·40	4·1	3·9	1·8	2·5	8·4	5·1	3·2	2·2	3·1	3·4
Nb	52	12	38	41	34	46	46	48	34	62	62	47	40	46	52
Sr	1415	437	1507	1624	735	1716	1559	1531	1555	1562	1626	1216	1836	1429	1913
Zr	394	102	252	279	223	254	212	291	277	498	365	303	268	278	358
Y	14·5	12·5	18·4	18·8	21·9	17·6	16·9	23·3	21	15·9	13·0	15·9	9·2	17·6	29·2
$(^{87}Sr/^{86}Sr)_m$	0·70788 (1)	0·71018 (1)	0·70769 (1)	0·70737 (2)	0·70761 (1)	0·70738 (1)	0·70702 (1)	0·70768 (1)	0·70731 (2)	0·70712 (2)		0·70783 (3)	0·70758 (1)	0·70763 (1)	
$(^{143}Nd/^{144}Nd)_m$		0·51189 (1)	0·51167 (1)	0·51192 (1)	0·51182 (1)	0·51166 (1)	0·51191 (1)	0·51194 (1)	0·51190 (1)	0·51187 (1)		0·51194 (1)	0·51197 (1)	0·51191 (1)	
$(^{87}Sr/^{86}Sr)_i$	0·70717	0·70612	0·70722	0·70700	0·70712	0·70695	0·70680	0·70724	0·70704	0·70677		0·70745	0·70727	0·70724	
$(^{143}Nd/^{144}Nd)_i$		0·51180	0·51159	0·51184	0·51174	0·51159	0·51183	0·51186	0·51181	0·51178		0·51185	0·51187	0·51183	

Table 1: continued

	16	17	18	19	20	21	22	23	24	25	26	27	28	29	30
Locality:	Mbocayaty	Potrero Ybaté	Sapucai	Acahay	Cerro Santo Tomás	Cerro San José	Cerro Arrúa-í	Cerro Acahay	Cerro Ybypyté	Cerro Capiitindy	Sapucai	Ybytyruzú	Cerro Chobí	Cerro Boggiani	Fecho dos Morros
Suite:	AB–T, HK	AB–T, K	AB–T, K	AB–T, K	AB–T, K	AB–T, tK	AB–T, tK	AB–T, tK	AB–T, tK	AB–T, tK	AB–T, HK	AB–T, K	AB–T, tK	Na	Na
Rock type:	Syeno-gabbro	Nepheline syenodiorite	Syeno-gabbro	Alkaligabbro gabbro	Nepheline syenodiorite	Alkali gabbro	Nepheline syenodiorite	Trachy-basalt	Trachy-andesite	Trachy-phonolite	Trachy-basalt	Trachy-andesite	Trachy-phonolite	Nepheline syenite	Nepheline syenite
Sample:	47-PS263	113-PS228	142-PS30	208-3341	181-3090	103-PS237	256-PS201	199-3344	254-PS206	43-PS500	D159-PS9	D14-PS260	D46-PS256	CB 1-3	FDM5
wt %															
SiO_2	51·66	52·56	48·33	46·01	51·03	48·91	51·45	51·98	51·72	56·50	49·43	53·83	59·92	58·14	56·22
TiO_2	1·76	1·22	1·74	2·02	1·31	1·82	1·64	1·51	1·37	0·88	1·65	1·52	0·13	0·36	1·07
Al_2O_3	13·89	16·46	17·75	16·01	17·32	12·77	17·85	15·87	16·34	17·84	14·36	14·17	18·88	19·07	18·67
Fe_2O_3	3·30	2·23	3·02	3·64	3·02	3·03	1·96	3·94	4·56	2·28	3·81	2·52	1·00		
FeO	4·11	4·84	5·67	7·55	5·47	6·62	6·18	4·36	4·37	2·67	4·94	5·41	0·79	3·49*	5·38*
MnO	0·11	0·12	0·16	0·19	0·18	0·18	0·15	0·14	0·15	0·16	0·16	0·16	0·18	0·28	0·30
MgO	6·37	4·40	4·77	5·88	3·62	7·54	4·23	5·23	4·50	0·86	7·61	3·02	0·02	0·08	1·26
CaO	5·25	6·60	8·76	10·51	7·18	11·58	6·29	7·25	5·95	4·45	7·55	6·01	1·21	0·89	1·76
Na_2O	2·04	3·76	3·08	2·61	3·83	3·30	4·49	3·94	4·00	5·71	2·29	3·31	7·36	12·39	9·21
K_2O	8·13	5·16	4·14	2·88	4·52	2·16	3·99	3·83	3·10	5·59	5·72	6·34	6·61	5·27	5·18
P_2O_5	0·59	0·59	0·66	0·93	0·50	0·37	0·67	0·47	0·36	0·28	0·34	0·50	0·02	0·02	0·92
LOI	2·17	1·38	0·83	0·94	1·71	0·99	1·30	1·00	2·94	2·36	1·07	2·67	3·65		
Total	99·38	99·32	98·90	99·17	99·69	99·27	100·20	99·52	99·36	99·58	98·93	99·46	99·77	99·99	99·97
mg-no.	0·65	0·57	0·54	0·53	0·48	0·63	0·52	0·58	0·52	0·32	0·69	0·45	0·03	0·11	0·35

p.p.m.															
La	108	86	71	58	77	63	73	56	52	154	81	138	109	130	119
Ce	197	155	130	122	143	120	137	109	101	251	119	249	170	194	229
Pr			13·7	14·7				12·9			13·0			16·6	19·4
Nd	65	65·2	58·2	69·1	59·5	58·2	62·5	52·0	48·8	84·0	49·1	97	92	40·5	64·2
Sm	12·9	10·09	9·75	12·32	7·4	10·05	10·68	8·83	8·45	12·70	9·81	14·7	13	6·37	11·7
Eu	2·5	2·73	2·76	3·72	2·2	2·87	3·07	2·52	2·49	3·28	2·59	4·14		1·54	1·2
Gd	4·3	6·79	7·13	8·88	4·6	7·25	7·50	6·16	5·82	5·70	4·71	7·48		8·42	11·8
Tb			0·85	1·06				0·77			0·65			1·11	1·18
Dy	3·5	3·35	4·06	4·82	3·9	3·84	4·51	3·64	3·39	5·44	3·40	5·74		6·82	4·48
Ho			0·72	0·80				0·65			0·64			1·56	0·73
Er	1·2	1·51	1·97	1·83	1·5	1·65	1·90	1·52	1·50	2·59	1·70	2·54		5·78	2·70
Tm			0·28	0·26				0·24			0·27			1·08	0·39
Yb	1·0	1·13	11·45	1·41	1·48	1·25	1·69	1·31	1·26	2·25	1·32	2·13		8·51	2·35
Lu	0·18	0·21	0·27	0·26	0·21	0·24	0·30	0·23	0·24	0·35	0·19	0·27		1·22	0·30
Cr															
Ni	429	106	37	57	22	153	27	1163	10	5	376	24	2	2	4
Rb	131	39	15	33	13	47	18	47	2	7	81	16	2	8	8
Ba	162	97	116	53	100	41	70	92	56	77	119	114	167	299	156
Th	1995	1426	1268	1003	1186	729	1021	1117	1050	2684	1334	1515	167	98	901
U	9·8	10·5	6·9	3·4	11·9	6·7	12·4	7·2	8·6	21·8	32·2	18·6		20·1	5·3
Ta	3·1	2·4	2·2	0·8	2·3	1·7	2·4	1·1	1·4		7·4			44·6	9·4
Nb	3·2	2·2	1·4	1·8	4·4	1·5	1·9	2·3	1·7		1·1			27·1	29·6
Sr	48	36	26	16	41	28	36	31	27	59	37	63	84	436	277
Zr	1618	1834	1853	2057	1378	1527	1489	1224	1153	1956	1163	964	625	135	741
Y	282	262	213	224	261	282	291	255	239	474	268	459	952	3418	1436
	19	15·3	19·2	21·9	18·0	17·5	22·2	17·4	16·0	29	19·3	26	9	42	54
$(^{87}Sr/^{86}Sr)_m$	0·70787 (1)	0·70751 (1)	0·70749 (2)	0·70729 (1)	0·70771 (1)	0·70728 (1)	0·70708 (2)	0·70767 (2)	0·70763 (1)	0·70750 (2)	0·70778 (1)	0·70778 (4)	0·70894 (6)	0·72800 (1)	0·70562 (1)
$(^{143}Nd/^{144}Nd)_m$	0·51171 (1)		0·51182 (1)	0·51188 (1)	0·51190 (1)				0·51182 (1)	0·51171 (1)	0·51175 (1)	0·51180 (2)	0·51168 (2)	0·51222 (1)	0·51241 (1)
$(^{87}Sr/^{86}Sr)_i$	0·70734	0·70723	0·70716	0·70715	0·70733	0·70714	0·70683	0·70727	0·70737	0·70729	0·70724	0·70716	0·70753	0·70570	0·70350
$(^{143}Nd/^{144}Nd)_i$	0·51161		0·51175	0·51179	0·51184				0·51173	0·51163	0·51165	0·51172	0·51154	0·51207	0·51223

Table 1: continued

	31	32	33	34
Locality:	Ñemby	Cerro Patiño	Estancia Guavira-y	Estancia Ramirez
Suite:	Na	Na	Na	Na
Rock type:	Nephelinite	Nephelinite	Nephelinite	Nephelinite
Sample:	273-3209	262-3399	PS-569	PS570
wt %				
SiO_2	42·51	42·42	42·29	44·68
TiO_2	2·05	2·32	3·67	3·04
Al_2O_3	13·41	14·40	13·53	14·80
Fe_2O_3	4·02	3·99		
FeO	6·48	6·13	11·86*	12·18*
MnO	0·20	0·17	0·19	0·23
MgO	9·54	9·77	8·88	5·41
CaO	10·45	11·71	11·52	10·46
Na_2O	5·80	5·00	5·83	6·90
K_2O	1·46	0·67	1·30	1·32
P_2O_5	1·18	0·87	0·73	0·77
LOI	2·19	1·87		
Total	99·29	99·32	99·80	99·79
mg-no.	0·67	0·68	0·61	048
p.p.m.				
La	119	81	71	98
Ce	186	145	132	176
Pr				
Nd	63·7	43·4	60·9	88
Sm	11·23	8·15	10·4	15·0
Eu	2·15	1·89	1·9	2·69
Gd	5·16	5·77	4·59	6·42
Tb	0·75		0·81	1·13
Dy	4·21	4·81	4·62	6·35
Ho				
Er	2·75	2·13	2·56	3·49
Tm				
Yb	1·79	1·65	1·60	2·17
Lu	0·27	0·23	0·23	0·31
Cr				
Ni	648	542	311	35
Rb	273	207	128	30
Ba	59	22	91	58
Th	980	1090	878	904
U	11·0	10·5		
Ta	2·4	2·3		
Nb	7·1	5·9		
Sr	101	89	72	101
Zr	1013	1016	951	1446
Y	234	165	289	420
	33	26	33	46
$(^{87}Sr/^{86}Sr)_m$	0·70374 (1)	0·70395 (1)	0·70482 (3)	0·70544 (4)
$(^{143}Nd/^{144}Nd)_m$	0·51276 (1)	0·51275 (1)	0·51250 (1)	0·51233 (2)
$(^{87}Sr/^{86}Sr)_i$	0·70363	0·70391	0·70435	0·70524
$(^{143}Nd/^{144}Nd)_i$	0·51273	0·51272	0·51242	0·51225

* Total Fe as FeO; *mg*-no. = atomic Mg/(Mg + Fe^{2+}), assuming Fe_2O_3/FeO = 0·18.
1–28: potassic rocks from ASU; 29–34: sodic rocks (29 and 30, from Alto Paraguay; 31 and 32, from ASU; 33 and 34, from San Juan Bautista). $^{87}Sr/^{86}Sr$ and $^{143}Nd/^{144}Nd$ isotopic ratios were measured on a MAT 262 multicollector mass spectrometer (Ludwig, 1987). The average value of NBS 987 during data acquisitions was 0·71026 ± 0·00002 (2σ), $^{86}Sr/^{88}Sr$ normalized to 0·1194. La Jolla standard gave 0·511856 ± 0·000015 (2σ). Nd isotopic ratios were normalized for within-run fractionation to $^{146}Nd/^{144}Nd$ = 0·7219.

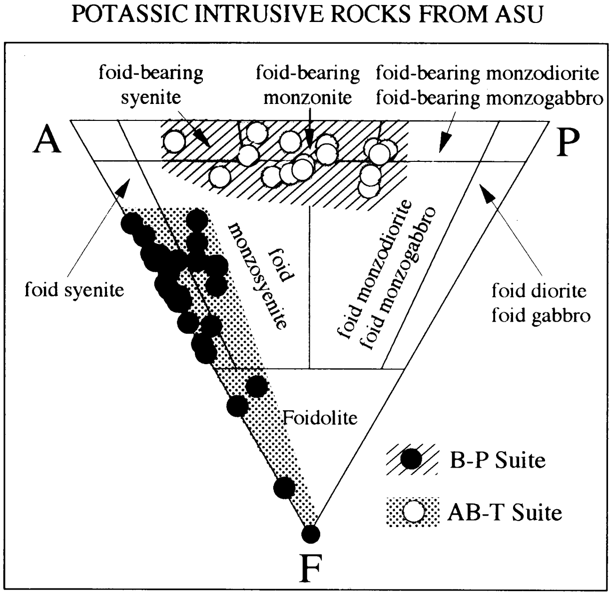

Fig. 3. QAPF diagram (Streckeisen, 1976) for selected samples of ASU intrusive potassic rocks. B–P, basanite–phonolite suite; AB–T, alkali basalt–trachyte suite.

K and tK rocks. Variant textures include cumulitic clinopyroxene with alkali feldspar + nepheline + carbonate as intercumulus phases.

Basanites, tephrites and phonotephrites typically show porphyritic textures with phenocrysts of clinopyroxene ($Wo_{40-50}Fs_{10-19}$), olivine (Fo_{60-85}) and leucite pseudomorphed by sanidine + nepheline, in glassy groundmass containing microlites of clinopyroxene ± olivine, Ti-magnetite ± ilmenite, Ti-phlogopite–biotite, alkali feldspar (Or_{15-88}), nepheline–analcime ($Ne_{44-59}Ks_{17-26}$). Phenocrystal plagioclase (up to An_{74}) is present in K and tK rocks. Accessory phases are amphibole (pargasite–kaersutite), apatite ± zircon.

Phonolites are characterized by phenocrysts of leucite pseudomorphs, alkali feldspar (Or_{47-75}), clinopyroxene ($Wo_{48-50}Fs_{11-34}$), Fe-pargasite, nepheline ± biotite ± sphene ± melanite (Ti-andradite up to 68 wt %) ± magnetite or haematite. Glassy groundmass contains microlites of alkali feldspar, nepheline, clinopyroxene ± Ti-andradite ± magnetite or haematite.

AB–T suite

Alkali gabbros, syenogabbros and syenodiorites are usually porphyritic and seriate. They contain clinopyroxene ($Wo_{43-50}Fs_{6-14}$), olivine (Fo_{43-82}), Ti-biotite, Ti-magnetite ± ilmenite, plagioclase (An_{31-78}), alkali feldspar (Or_{60-84}) and interstitial nepheline–analcime (Ne_{37-82} Ks_{15-23}) and alkali feldspar (Or_{80-97}). Accessories are apatite ± amphibole ± sphene ± zircon.

Nepheline syenites and syenites are equi- to subequigranular and seriate. The rock types are characterized by alkali feldspar (Or_{32-63}), clinopyroxene ($Wo_{43-48}Fs_{10-32}$), nepheline (Ne_{85}) and hastingsite. Common accessories include sphene, apatite ± carbonate ± zircon.

Alkali basalts, trachybasalts and trachyandesites are porphyritic rocks characterized by phenocrysts and/or microphenocrysts of clinopyroxene ($Wo_{44-49}Fs_{7-15}$), olivine (Fo_{65-83}), plagioclase (An_{28-76}), magnetite, biotite in glassy groundmass containing microlites of clinopyroxene ($Wo_{46-49}Fs_{13-18}$), magnetite, ilmenite, biotite, plagioclase (An_{20-45}), alkali feldspar (Or_{52-65}), nepheline–analcime ($Ne_{37-73}Ks_{22-38}$), amphibole, apatite ± sphene ± zircon.

Trachyphonolites and trachytes are porphyritic to aphyric. The phenocrysts are alkali feldspar (Or_{60-65}) ± clinopyroxene ($Wo_{46-49}Fs_{14-20}$) ± plagioclase (An_{14-16}), pseudomorphed leucite, amphibole and biotite in hypocrystalline to glassy groundmass containing microlites of alkali feldspar, biotite, clinopyroxene ± biotite ± amphibole ± magnetite ± Ti-andradite ± haematite.

PETROCHEMISTRY

Chemical analyses were obtained by X-ray fluorescence (XRF) and by techniques described by Piccirillo & Melfi (1988). Representative specimens from B–P and AB–T suites are given in Table 1. A complete set of bulk-rock analyses has been given by Comin-Chiaramonti & Gomes (1996). Rare earth elements (REE), Th, U and Ta of selected specimens were determined by inductively coupled mass spectrometry (ICP-MS) (Alaimo & Censi, 1992) (Table 1). Close similarities in major, minor (not shown) and some trace elements (Fig. 4) are obvious on inspection. $[REE]_{CN}$ plots of intrusives, lavas and dykes from B–P and AB–T, respectively, are illustrated in Fig. 5. All specimens are similarly enriched in REE and exhibit steep, subparallel light REE (LREE) trends ($[La/Lu]_{CN}$ = 26–161, 17–62 and 11–46 for B–P, AB–T and Na rocks, respectively, which tend to flatten out for heavy REE (HREE) ($[Dy/Lu]_{CN}$ = 1·24–1·96, 1·09–2·00 and 0·56–2·05 for B–P, AB–T and Na rocks, respectively), HK dykes excepted. REE profiles with LREE enrichment and flat HREE suggest mantle sources which have been previously depleted by melt extraction and subsequently enriched (e.g. McKenzie & O'Nions, 1995).

The kamafugitic rocks from Alto Paranaíba Igneous Province (APIP; Gibson *et al.*, 1995*b*) from southern Brazil are distinct from the potassic rocks of eastern Paraguay in their higher LREE and MREE contents. APIP kamafugites have $[La/Lu]_{CN}$ ratios (69–173) falling in the upper range of the potassic B–P rocks. Multi-elemental diagrams, normalized to a primordial mantle

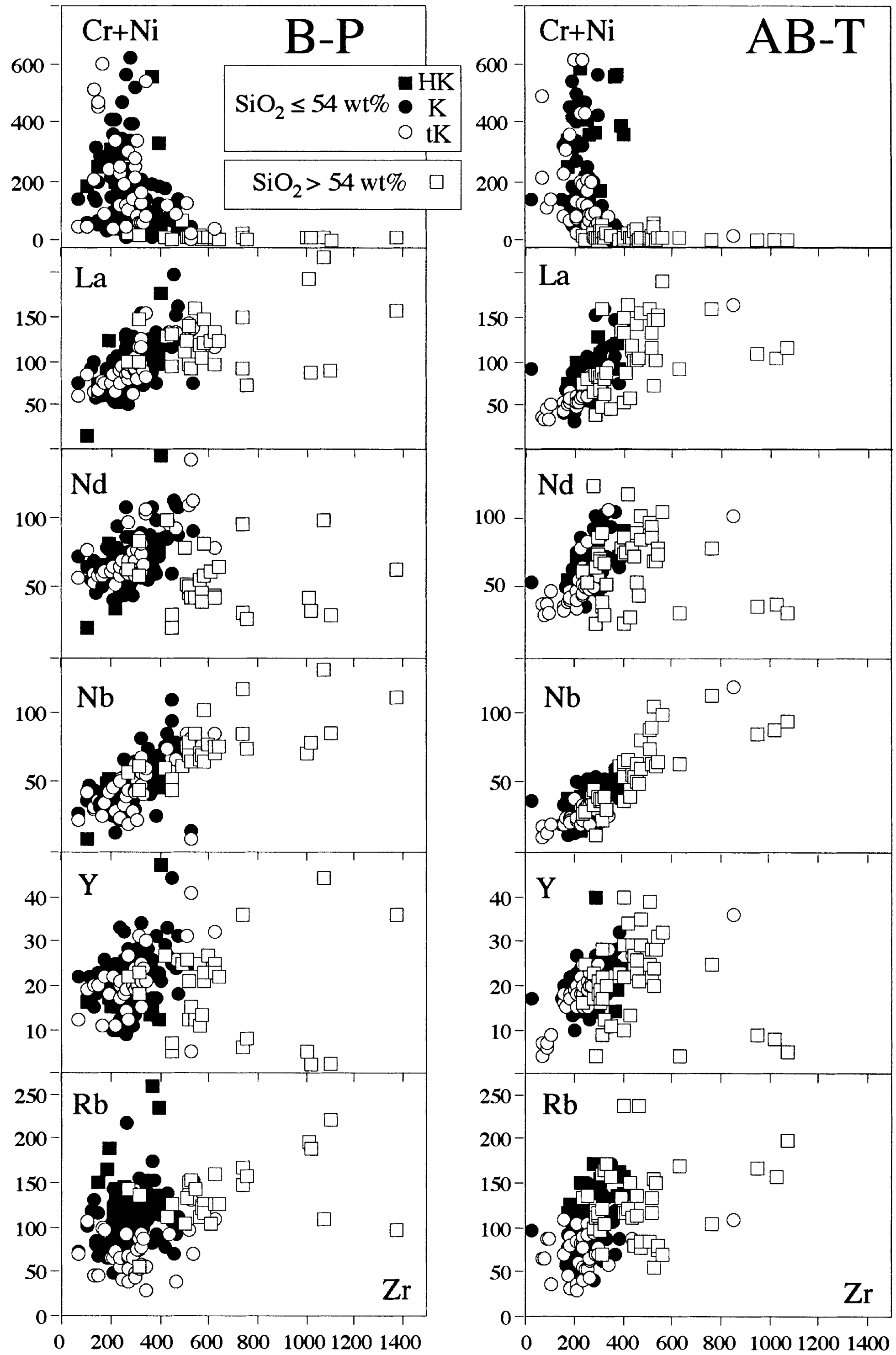

Fig. 4. Plots of Zr vs selected trace elements (p.p.m.) for the B–P and AB–T suites (intrusive rocks + lava flows + dykes). Abbreviations as in Fig. 3.

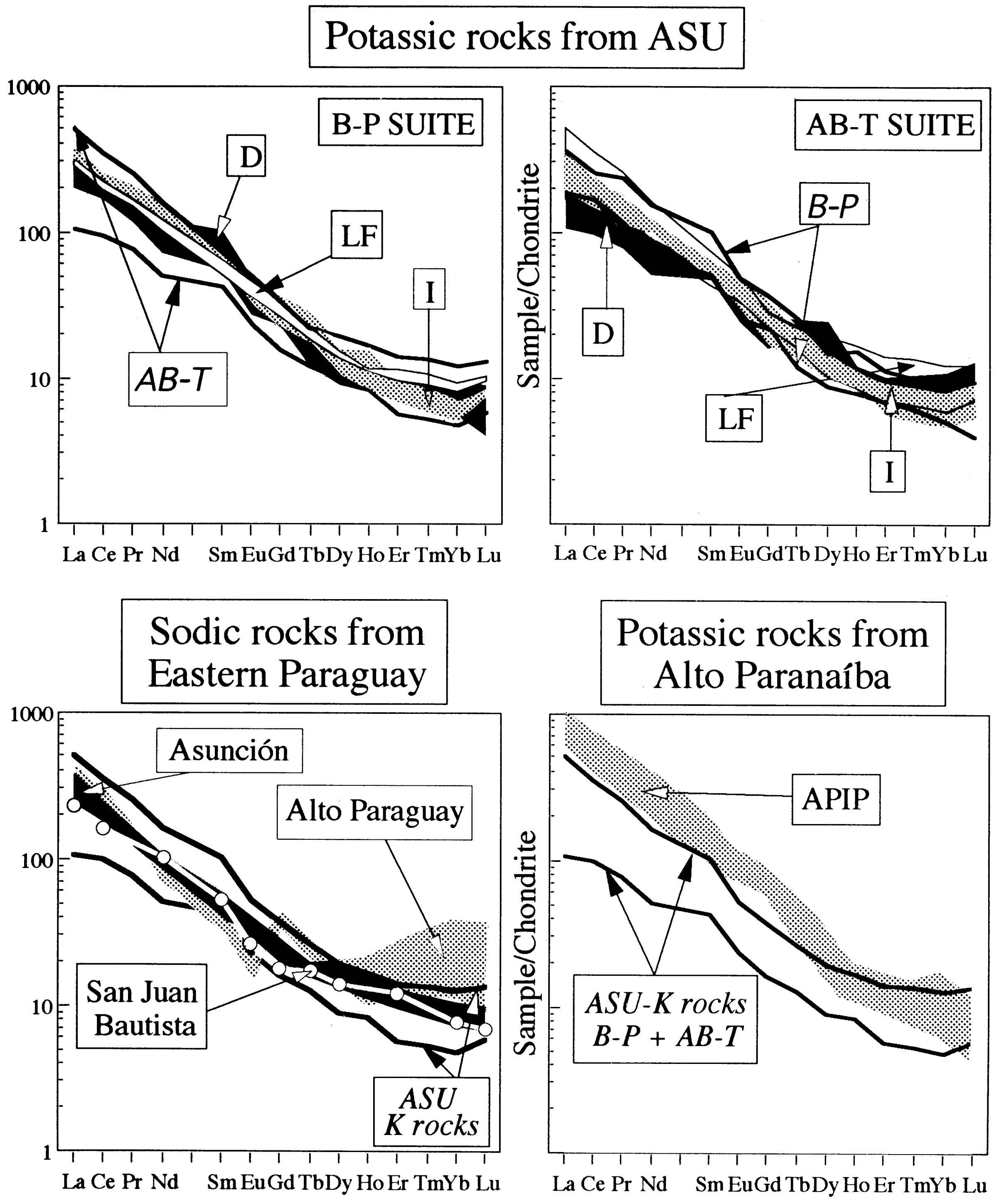

Fig. 5. Chondrite-normalized REE diagram for representative compositions of the B–P (basanite–phonolite) and AB–T (alkali basalt–trachyte) potassic suites, and Na rocks from eastern Paraguay (D, dykes; LF, lava flows; I, intrusives). APIP, Alto Paranaíba Igneous Province (Gibson *et al.*, 1995*b*) is also shown. Chondrite normalizing values are from Boynton (1984).

composition (Fig. 6), show a substantial overlap of B–P and AB–T compositions, negative Nb, Ta, P, Ti and Y spikes, and positive U, K and Sr spikes. Ta, Nb and Ti depletions yielded negative 'Ta–Nb–Ti anomalies', interpreted by some (e.g. Pearce, 1983) as characteristic of magmas generated in subduction-related environments. In general, B–P compositions are higher in Rb, K, Zr, Hf, Ti, Y, LREE and MREE than AB–T compositions. By contrast, the rocks of the Na suite yielded La/Nb and La/Ta ratios close to unity, respectively, whereas the Nb/K and Ta/K ratios are >1·0, respectively. It is of interest that the APIP potassic rocks show patterns similar to those of Na rocks from eastern Paraguay and are, therefore, distinct from those of the potassic B–P and AB–T suites. Notably, the variations of incompatible elements of the AB–T compositions mimic those of the SGF high-Ti (and low-Ti) tholeiitic basalts, which approach the lower (Rb to Nd) and higher (Sm to Lu) elemental concentrations of that suite (Fig. 6). Both SGF high- and low-Ti tholeiites and the ASU rocks fall out of the field for non-subduction related compositions in the Th/Zr vs Nb/Zr and Th/Yb vs Ta/Yb diagrams, respectively (Fig. 7). Consistent with the behaviour of Ta and Nb, the investigated Na and APIP rocks fall in the field where rocks are believed to be unrelated to subduction.

In summary, substantial overlap in bulk-rock chemistry exists between the investigated B–P and AB–T rocks, both characterized by variable K/Na ratio, but K types are dominant. REE and other incompatible elements show similar concentration levels and variation trends in the two suites. The mantle normalized incompatible element patterns of both ASU suites show strong affinities, including negative 'Ta–Nb–Ti anomalies', with the Paraná tholeiites. It seems significant that the sodic rocks show a slight positive anomaly for the latter elements (Comin-Chiaramonti *et al.*, 1991, 1992), similar to that of APIP potassic rocks (Gibson *et al.*, 1995*b*).

Sr–Nd isotopes

Typical specimens from the ASU K suite yielded initial (128 Ma) $^{87}Sr/^{86}Sr$ (Sr_i) and $^{143}Nd/^{144}Nd$ (Nd_i) isotopic ratios within the ranges 0·70612–0·70754 and 0·51154–0·51184, respectively. These are distinct from the values obtained for the Na rocks, i.e. ASU, Sr_i = 0·70362–0·70392 and Nd_i = 0·51259–0·51277; San Juan Bautista, Sr_i = 0·70435–0·70524 and Nd_i = 0·51225–0·51242; Alto Paraguay: Sr_i = 0·70350–0·70570 and Nd_i = 0·51207–0·51223. In the conventional ε_tSr vs ε_tNd isotope diagram (Fig. 8) the selected K specimens have higher Sr_i and lower Nd_i values with respect to the 'Low Nd' array of Hart *et al.* (1986), whereas the Na specimens approach bulk-Earth (BE) values, varying from depleted to enriched quadrants. The Amambay potassic rocks (Comin-Chiaramonti *et al.*, 1995) fall on the same general line of the ASU K rocks, but trending to more radiogenic Sr. Likewise, the sodic rocks from Alto Paraguay fall virtually on the same trend of the ASU analogues (San Juan Bautista). The latter approach the generalized field of the Paraná tholeiites from eastern Paraguay, which appear to fall at higher ε_tSr. The radiogenic Sr and Nd are, therefore, crucial in accounting for the source characteristics of the investigated rocks. Model contamination of the melts with crustal material implies unrealistic (up to 50%) contaminant fractions. Likewise, AFC processes do not account for the ASU isotope data, given the poor correlations (not shown) between large ion lithophile elements (LILEs) and Sr_i and Nd_i. Whole-rock $\delta^{18}O$ data from ASU K rocks (Marzoli, 1991) yielded +5·45 to +5·91‰ (V-SMOW), consistent with constituent clinopyroxene (+5·09 to +5·20‰) and biotite (+4·85 to +5·54‰) and expected mantle values. In summary, the data presented support the view that the Na rocks, close to BE, and the associated ASU K rocks, typically high in radiogenic Sr world-wide, represent the range of virtually uncontaminated source magmas from this region.

Nd-model ages for ASU K rocks (depleted mantle: T^{DM}) range from 1·4 to 2·0 Ga (mean 1·5 ± 0·2 Ga) whereas Na rocks yielded 0·5–0·8 (ASU), 1·0 (Alto Paraguay) and 0·8–0·9 Ga (San Juan Bautista). In general, high-Ti and low-Ti tholeiites from Paraná Basin (H-Ti and L-Ti, respectively) show mean T^{DM} 1·1 ± 0·1 and 1·5 ± 0·2 Ga, respectively. The range of model ages estimated for the potassic rocks implies that the corresponding melts derived from subcontinental mantle sources enriched by 'metasomatic processes' (see below) from Middle to Late Proterozoic. These calculations require that Sm/Nd fractionation was not significant during magma genesis.

PETROGENESIS

Evolution of the B–P and AB–T suites

Textural, mineralogical and petrochemical evidence points to fractional crystallization as potentially important in the evolution of the ASU suites. Mass balance calculations based on major oxides revealed that the evolution of both B–P and AB–T suites is compatible with fractional crystallization (Table 2). It should be noted that the corresponding Rayleigh's trace element fractionation for the B–P suite yielded observed/calculated ratios within the range 0·8–1·4, Ni and Ba in phonolite excepted. Likewise, trace element modelling for the AB–T suite yielded observed/calculated ratios of 0·8–1·2, except for Ni, Ba, Zr and Nb in the more evolved compositions.

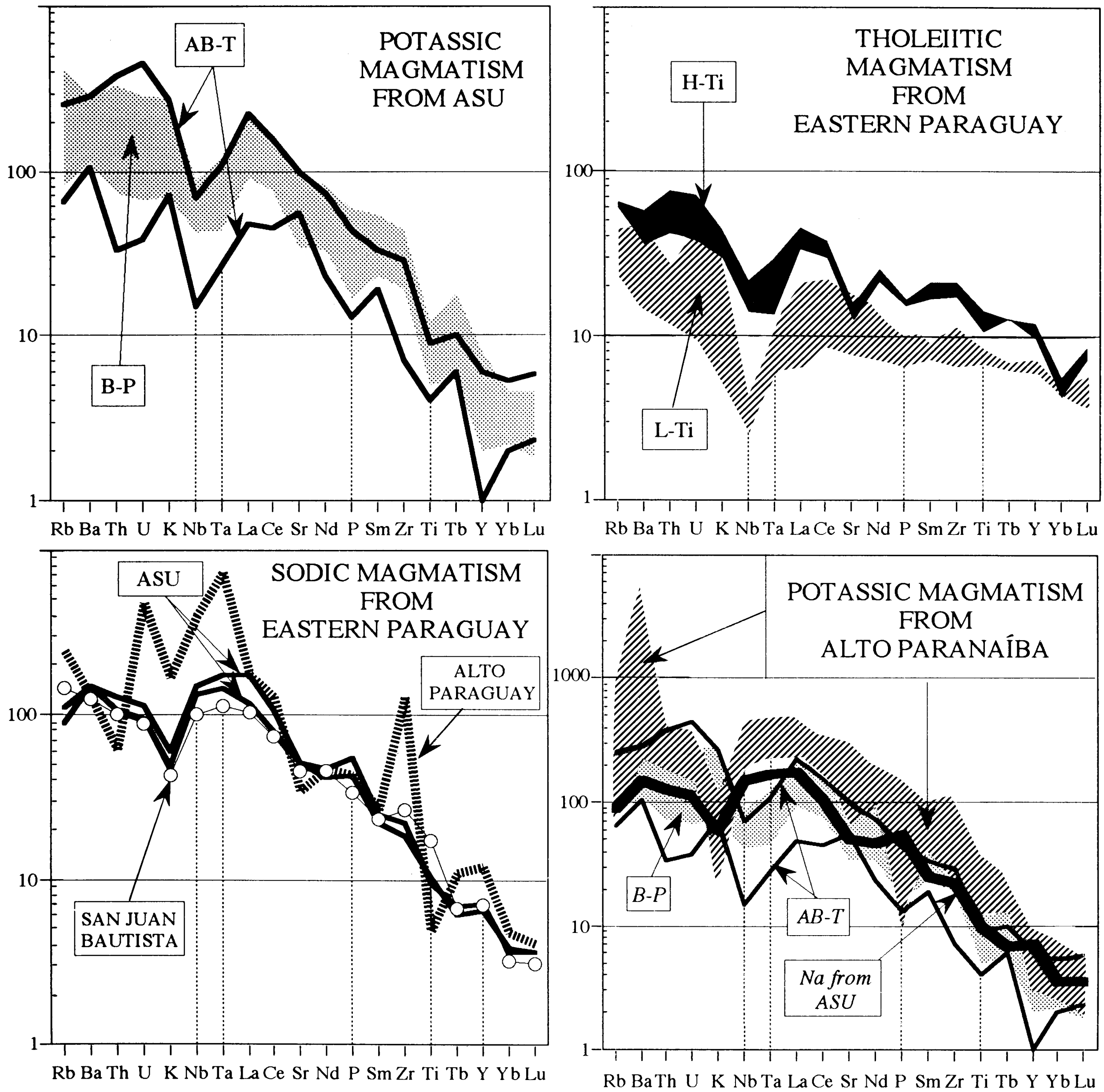

Fig. 6. Trace-element data normalized to primitive mantle [values from Sun & McDonough (1989)] for B–P (basanite–phonolite) and AB–T (alkali basalt–trachyte) suites from ASU, compared with sodic rock-types from Alto Paraguay and from southeastern Paraguay, with high-Ti and low-Ti tholeiites from eastern Paraguay and with potassic rock-types from northeastern Paraguay and Alto Paranaíba Igneous Province. Data source: Comin-Chiaramonti *et al.* (1991, 1992, 1995; Table 1) and Gibson *et al.* (1995*b*).

In an attempt to evaluate the role of fractionation in the B–P and AB–T suites, the variation of Th, Zr, Ni and Cr in the basanite to tephrite and alkali basalt to trachybasalt transitions, respectively, were investigated by means of a model elemental distribution, predicted for open-system fractionation in a periodically replenished magma reservoir (PRF; O'Hara & Mathews, 1981). Convergence of X and Y values was obtained, particularly for B–P. Similar results were obtained for the proposed tephrite to phonotephrite and trachybasalt to trachyandesite transitions, respectively. The general tendency for $X+Y$ values to approach unity suggests that the

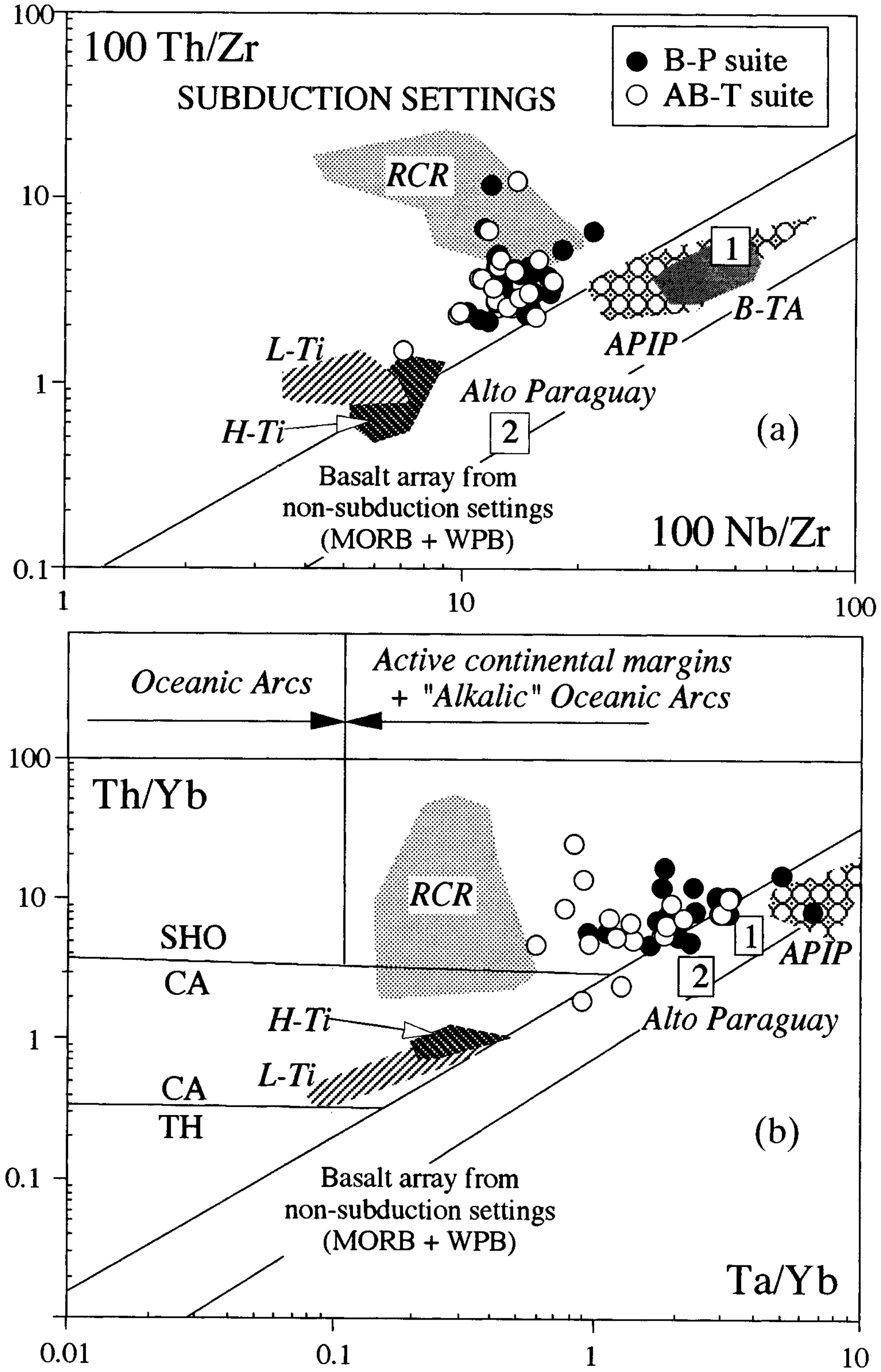

Fig. 7. (a) 100 × Nb/Zr vs 100 × Th/Zr ratios in typical compositions from eastern Paraguay potassic rock types (Table 1); the field of the Roman region lavas (RCR; Beccaluva *et al.*, 1991); Toro-Ankole lavas (B-TA, Mitchell & Bergman, 1991); APIP, Alto Paranaíba Igneous Province, southern Brazil (Gibson *et al.*, 1995*b*); tholeiitic basalts from the Paraná Basin: 'high-Ti', H-Ti and 'low-Ti', L-Ti, respectively, with initial ($^{87}Sr/^{86}Sr$)<0·7060 (Marques *et al.*, 1989), the average compositions of Na ankaratrites (1) from central–eastern Paraguay (Comin-Chiaramonti *et al.*, 1995) and (2) Alto Paraguay sodic rocks (unpublished data). (b) Ta/Yb vs Th/Yb. CA, calc-alkaline; SHO, shoshonitic; TH, tholeiitic boundaries for arc basalts are from Pearce (1983).

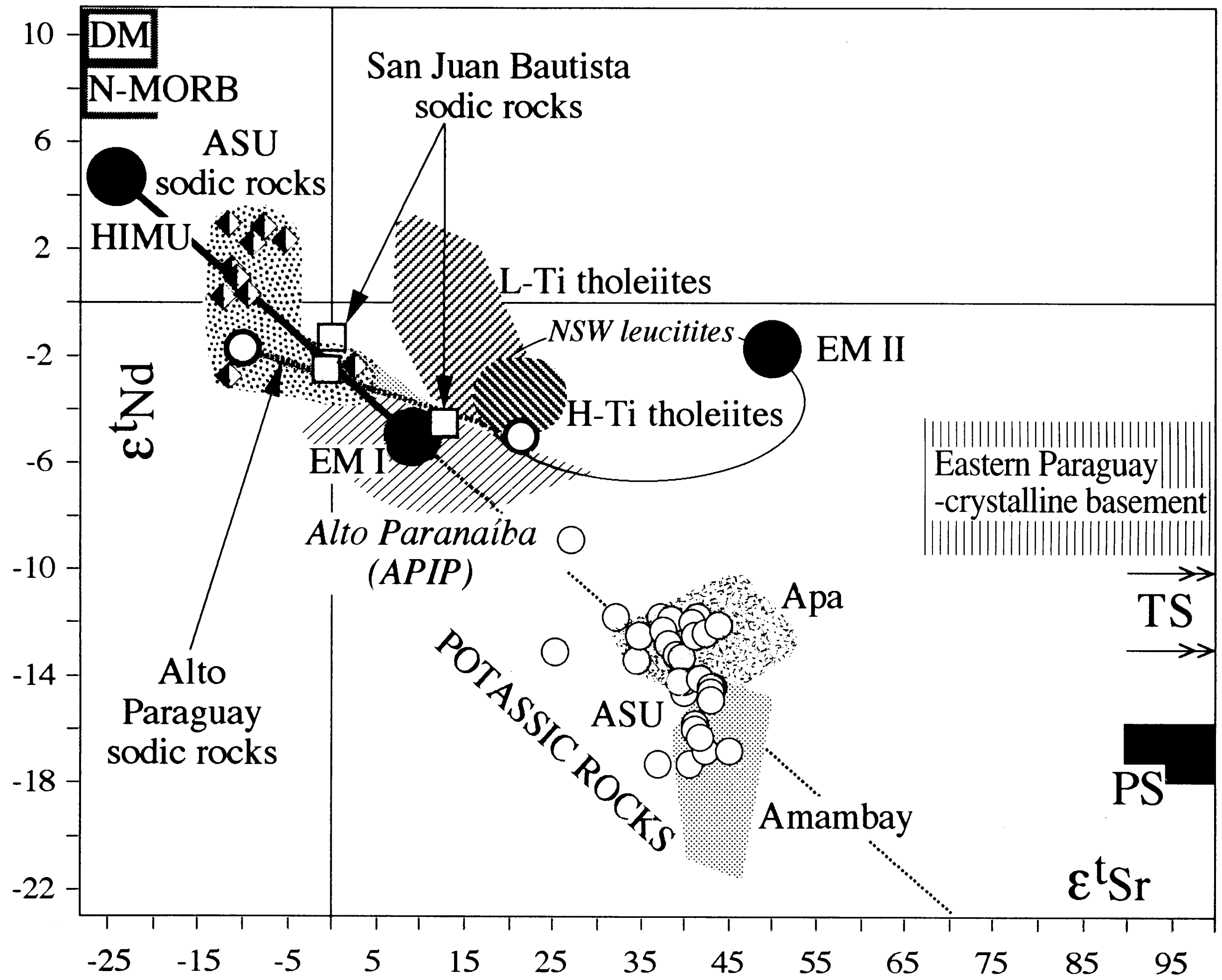

Fig. 8. ε_tSr vs ε_tNd correlation diagram for igneous rocks from eastern Paraguay. Data source: Piccirillo & Melfi (1988); Comin-Chiaramonti *et al.* (1991, 1992, 1995); Castorina *et al.* (1994, and unpublished data); Table 1. HIMU, EMI, EMII, terrigenous and pelagic sediments (TS and PS, respectively): Zindler & Hart (1986); New South Wales leucitites: Ewart (1989); Alto Paranaíba Igneous Province (APIP): Gibson *et al.* (1995*b*); crystalline basement: F. Castorina & P. Comin-Chiaramonti, unpublished data. The ε_tSr and ε_tNd values were calculated using the following values for bulk Earth: $^{87}Sr/^{86}Sr = 0{\cdot}7045$; $^{87}Rb/^{86}Rb = 0{\cdot}0827$; $^{143}Nd/^{144}Nd = 0{\cdot}512638$; $^{147}Sm/^{144}Nd = 0{\cdot}1967$.

PRF model is roughly equivalent to a succession of closed-system fractionation events. The phonotephrite to phonolite and trachyandesite to trachyte model fractionation, respectively, yielded negative values for Cr and Ni. Therefore, the extreme rock compositions are inconsistent with Rayleigh-type fractionation processes, probably reflecting, at least in part, their distinct $f(O_2)$ and its influence on partition coefficients.

Mantle source characteristics

The origin of the ASU alkaline magmas is closely related to and probably constrained by the geodynamic processes which promoted the generation of the adjacent and 'coeval' SGF tholeiites. The origin and emplacement of the latter basalts occurred before the opening of the South Atlantic and appears to be related to early stages of lithospheric extension, associated with an anomalously hot mantle (Piccirillo & Melfi, 1988; Hawkesworth *et al.*, 1988, 1992; Hergt *et al.*, 1991; Turner & Hawkesworth, 1995). The K/Na and trace element variations and Sr–Nd isotope characteristics of the ASU suites support the view that the lithospheric mantle played an important role in their genesis as well as that of the Paraná flood basalts (Piccirillo *et al.*, 1989; Gibson *et al.*, 1995*a*; Peate & Hawkesworth, 1996).

The most mafic ASU potassic basanites and alkali basalts are relatively evolved compared with expected primary compositions (e.g. *mg*-number >0·65, Ni >235 p.p.m.). Possible ASU primary melts (e.g. *mg*-number

Table 2: Crystal fractionation models; average major (wt %) and trace elements (p.p.m.) of potassic rocks from ASU (anhydrous basis; numbers in parentheses are standard deviations)

	B–P suite				AB–T suite				
	B ($n=3$)	T ($n=74$)	PT ($n=101$)	P ($n=23$)	AB ($n=8$)	TB ($n=52$)	TA ($n=65$)	TP ($n=20$)	TR ($n=15$)
SiO_2	48·86 (0·34)	49·36 (1·21)	50·85 (1·47)	54·28 (2·49)	50·72 (1·74)	51·43 (1·17)	53·53 (1·97)	58·58 (2·39)	60·91 (2·45)
TiO_2	1·55 (0·12)	1·79 (0·25)	1·65 (0·25)	1·04 (0·40)	1·53 (0·27)	1·51 (0·22)	1·50 (0·23)	0·83 (0·43)	0·94 (0·44)
Al_2O_3	13·30 (0·25)	15·17 (1·69)	16·68 (1·49)	19·48 (1·07)	12·99 (1·73)	15·62 (1·62)	17·20 (1·36)	19·04 (0·90)	18·24 (0·84)
FeO_t	9·33 (0·95)	9·60 (0·82)	8·67 (1·03)	5·41 (1·65)	9·11 (1·38)	8·75 (0·61)	7·88 (1·24)	4·22 (1·74)	4·26 (1·70)
MnO	0·17 (0·01)	0·17 (0·02)	0·17 (0·02)	0·15 (0·03)	0·17 (0·03)	0·16 (0·02)	0·15 (0·02)	0·14 (0·04)	0·12 (0·10)
MgO	8·54 (1·50)	6·25 (1·19)	4·44 (0·98)	1·56 (1·07)	8·63 (1·44)	6·04 (1·45)	3·84 (1·27)	1·14 (0·81)	1·34 (0·73)
CaO	10·86 (0·93)	9·26 (0·89)	7·54 (0·97)	4·63 (1·51)	9·86 (0·79)	8·46 (0·74)	6·34 (1·22)	3·47 (1·31)	2·28 (1·54)
Na_2O	3·40 (0·21)	3·33 (0·61)	4·02 (0·60)	6·05 (1·39)	2·60 (1·19)	3·31 (0·67)	3·76 (0·90)	5·60 (1·21)	4·21 (1·02)
K_2O	3·53 (0·60)	4·48 (0·88)	5·37 (1·12)	7·00 (1·14)	3·93 (1·05)	4·24 (1·07)	5·27 (1·44)	6·71 (0·93)	7·43 (1·86)
P_2O_5	0·46 (0·08)	0·59 (0·17)	0·61 (0·16)	0·40 (0·26)	0·46 (0·09)	0·49 (0·11)	0·55 (0·11)	0·27 (0·19)	0·31 (0·18)
Cr	388 (15)	161 (111)	70 (65)	16 (16)	316 (86)	165 (143)	64 (48)	8 (10)	10 (13)
Ni	140 (40)	51 (27)	34 (20)	6 (5)	91 (33)	59 (36)	24 (21)	6 (5)	8 (5)
Ba	1214 (4)	1470 (336)	1563 (357)	2022 (1104)	1444 (344)	1310 (265)	1417 (376)	1334 (811)	1140 (482)
Rb	61 (20)	90 (28)	107 (37)	129 (39)	77 (35)	89 (28)	104 (32)	131 (34)	136 (32)
Sr	1383 (150)	1703 (323)	1731 (441)	2443 (719)	1251 (185)	1496 (288)	1440 (353)	1358 (692)	815 (325)
La	73 (13)	85 (22)	97 (23)	126 (36)	65 (38)	72 (18)	87 (22)	114 (36)	93 (39)
Ce	136 (27)	153 (36)	171 (39)	205 (47)	124 (58)	126 (32)	153 (34)	185 (59)	159 (62)
Nd	58 (3)	67 (14)	76 (28)	84 (18)	52 (19)	53 (12)	66 (15)	64 (25)	64 (28)
Zr	162 (36)	258 (74)	299 (72)	531 (150)	210 (90)	224 (52)	295 (54)	541 (167)	440 (130)
Y	18 (4)	20 (5)	21 (5)	25 (9)	18 (5)	19 (4)	21 (4)	22 (10)	22 (10)
Nb	38 (7)	40 (12)	48 (15)	77 (21)	29 (14)	31 (8)	40 (9)	66 (26)	50 (23)
mg-no.	0·65	0·57	0·51	0·37	0·66	0·59	0·50	0·36	0·39

Table 2: continued

AB–T suite	Ol AB	Ol TB	Ol TA	Cpx AB	Cpx TB	Cpx TA	Biot AB	Biot TB	Biot TA	Amph TA	Mt AB	Mt TB	Mt TA	Pl TB	PlTA	AfTA	ApTA
SiO_2	39·98	39·43	38·42	49·57	51·00	51·39	39·92	40·12	38·11	41·54	0·16	0·12	0·05	48·79	54·71	65·25	0·16
TiO_2				1·70	1·33	1·25	8·23	6·97	7·88	4·64	17·33	24·14	19·26				
Al_2O_3				4·99	3·03	3·02	12·84	13·88	14·81	11·87	3·41	2·81	2·27	32·85	28·85	19·24	0·05
FeO_t	14·30	16·92	22·40	5·56	7·09	7·72	12·77	12·53	12·87	13·13	75·55	69·50	76·29		0·18	0·72	0·98
MnO	0·25	0·55	0·32	0·28	0·30	0·39	0·11	0·21	0·26	0·37	1·01	1·10	1·29				0·13
MgO	45·47	42·99	38·70	16·69	15·44	14·27	16·03	17·08	15·40	11·52	2·39	2·23	0·84				0·28
CaO		0·11	0·16	20·79	21·25	21·65	0·01	0·01	0·15	12·32	0·15	0·09		15·69	10· 83	0·64	55·43
Na_2O				0·42	0·54	0·30	0·36	0·01	0·27	2·69				2·49	5·26	5·50	0·05
K_2O				0·01	0·01	0·01	9·73	9·21	10·24	1·94				0·18	0·17	8·65	
P_2O_5																	42·93

B–P suite	Ol B	Ol T	Ol PT	Cpx B	Cpx T	Cpx PT	Biot T	Biot PT	Mt B	Mt T	Mt PT	Pl B	Pl T	Pl PT	Lc TY	Lc PT	Ap T	Ap PT
SiO_2	39·98	39·12	38·43	52·16	51·80	47·74	40·03	37·69	0·19	0·3	0·80	50·99	53·50	59·87	55·28	54·72	0·32	
TiO_2				1·09	0·98	1·42	8·98	6·29	23·93	18·19	18·23							
Al_2O_3				2·25	2·33	5·66	12·48	16·29	3·95	5·43	4·02	30·96	29·78	24·71	23·33	22·97	0·09	
FeO_t	14·33	18·57	22·29	5·85	7·15	7·73	12·47	14·60	68·78	73·74	75·71	0·37	0·18	0·24	0·19	0·50	0·37	1·59
MnO	0·26	0·37	0·51	0·10	0·19	0·18	0·12	0·12	0·56	1·03	0·85	0·01	0·01				0·04	0·22
MgO	45·23	41·69	38·53	16·20	15·48	12·42	15·69	14·90	2·56	1·32	0·34	0·27	0·01				0·01	0·56
CaO	0·24	0·25	0·24	22·28	21·63	24·43	0·01	0·01	0·07	0·05	0·05	13·92	11·89	6·74	0·24	0·08	55·89	54·78
Na_2O				0·07	0·43	0·42	0·96	9·23				3·29	4·45	6·70	1·29	0·66	0·10	
K_2O					0·01	0·01	9·27	9·86				0·13	0·18	1·73	19·67	21·06	0·01	
P_2O_5																	43·17	42·84

Table 2: continued

	B–P suite				AB–T suite								
	B→T		T→PT	PT→P	AB→TB		TB→TA		TA→TP			TA→TR	
	(a)	(b)			(a)	(b)	(a)	(b)	(a)	(b)	(c)	(a)	(b)
F (%)	82·69	84·42	72·56	42·49	80·86	81·48	77·46	75·20	66·80	70·03	73·01	52·34	53·18
Ol	14·86	16·31	1·80	8·71	14·17	15·97	12·15		4·86	11·38		4·46	
Cpx	74·00	80·94	49·62	30·32	78·56	79·92	53·70	57·30	33·95	27·18	37·27	7·50	11·96
Biot			13·06		3·58			17·17	15·56		20·78		6·09
Amph										13·31		31·88	31·85
Mt	1·58	2·74	8·48	9·29	3·69	4·11	8·35	6·59	11·54	12·68	11·13	7·43	7·30
Pl	9·56		22·46	34·66			25·80	18·93	32·36	32·49	29·96	29·66	28·61
Af												16·18	12·12
Lc			3·81	16·08									
Ap			0·76	0·93					1·73	2·95	0·87	2·88	2·08
ΣR^2	0·545	0·725	0·155	0·007	0·649	0·655	0·153	0·428	0·645	0·974	0·730	0·430	0·541

Mass balance calculations based on major elements [the numbers are the amounts (wt %) of the phases constituting the mineral assemblage subtracted from the parent liquid].

	Ol	Cpx	Biot	Amph	Mt	Pl	Af	Lc	Ap
Cr	0·72	5·69	1·00	8·00	7·70	0·03	0·01	0·06	0·01
Ni	30·71	2·00	8·00	6·40	6·54	0·03	0·01	0·06	0·01
Ba	0·04	0·07	10·00	0·61	0·14	0·24	3·02	0·18	0·95
Rb	0·08	0·10	3·00	0·15	0·23	0·03	0·42	0·44	0·56
Sr	0·01	0·33	0·20	1·01	0·23	2·12	4·11	0·02	1·67
La	0·01	0·22	0·02	0·56	0·53	0·12	0·46	0·02	5·16
Ce	0·01	0·34	0·02	0·87	0·56	0·14	0·36	0·02	6·34
Nd	0·01	0·68	0·03	1·82	0·55	0·07	0·31	0·02	6·60
Zr	0·05	0·10	0·08	0·80	0·35	0·01	0·13	0·01	0·01
Y	0·01	0·77	0·80	2·88	0·55	0·05	0·24	0·01	5·08
Nb	0·01	0·14	0·30	0·89	3·86	0·01	0·12	0·02	0·09

Mineral–liquid partition coefficients, Marzoli (1991) and Caroff *et al.* (1993).

Table 2: continued

	B–P suite				AB–T suite								
	T (a)	T (b)	PT	P	TB (a)	TB (b)	TA (a)	TA (b)	TP(a)	TP(b)	TP(c)	TR(a)	TR(b)
Cr	0·80	0·81	1·02	0·73	1·20	1·18	0·79	0·90	0·29	0·32	0·25	0·84	0·95
Ni	0·97	0·98	1·21	1·20	1·34	1·39	1·87	1·07	0·90	1·35	0·50	2·41	1·38
Ba	1·02	0·97	1·21	0·69	0·80	0·75	0·86	1·36	1·24	0·72	1·37	0·70	1·56
Rb	1·24	1·27	1·01	0·64	0·98	0·96	0·93	1·04	1·05	0·92	1·33	0·76	0·91
Sr	1·11	1·09	0·93	1·29	1·03	1·03	0·90	0·86	0·90	0·93	0·90	0·90	0·79
La	1·00	1·02	0·91	0·72	0·93	0·94	0·99	0·96	0·98	1·08	1·03	0·77	0·75
Ce	0·98	1·00	0·93	0·69	0·87	0·88	1·01	0·98	0·93	1·01	0·97	0·82	0·79
Nd	1·05	1·07	0·98	0·68	0·93	0·93	1·08	1·06	0·77	0·88	0·80	0·93	0·91
Zr	1·34	1·37	0·87	0·89	0·88	0·89	1·04	1·02	1·27	1·37	1·38	0·96	0·97
Y	1·03	1·05	0·94	0·74	1·00	1·00	0·97	1·00	0·88	0·99	0·92	1·20	1·22
Nb	0·90	0·92	1·00	1·03	0·91	0·92	1·11	1·08	1·37	1·46	1·43	0·97	0·98

Trace elements, observed/calculated ratios (Rayleigh fractionation).
B–P suite: B, basanite; T, tephrite; PT, phonotephrite; P, phonolite. AB–T suite: AB, alkali basalt; TB, trachybasalt; TA, trachyandesite; TP, trachyphonolite; TR, trachyte. n, number of samples, *mg*-no. = atomic $Mg/(Mg+Fe^{2+})$, assuming $Fe_2O_3/FeO = 0{\cdot}18$. Mineral compositions used in mass balance calculations (see text): Ol, olivine; Cpx, clinopyroxene; Biot, biotite; Amph, amphibole; Mt, magnetite; Pl, plagioclase; Af, alkali feldspar; Lc, leucite; Ap, apatite. Data source: Comin-Chiaramonti & Gomes (1996). F (%), weight fraction of residual liquid. ΣR^2, sum of the squared residuals.

~0·74) in equilibrium with Fo_{90-91} are expected to have fractionated olivine (Ol) and clinopyroxene (Cpx) at or near the mantle source and certainly during the ascent to the surface. Neglecting the effects of polythermal–polybaric fractionation on the chemistry of the fractionates, notional crystal fractions have been calculated to restore the selected ASU parental compositions to possible near-primary melts in equilibrium with their mantle sources (Table 3).

The strong LREE/HREE ratios of the primary melt compositions of ASU and Alto Paranaíba [$(La/Lu)_{CN}$ = 28–54 and 113, respectively] require melting of peridotite sources with unrealistically high proportions of garnet in the solid residua. Notionally, for 3% batch melting (see below) the garnet proportions in the ASU and Alto Paranaíba peridotite residua are higher than 14 wt %.

Mass balance calculations, starting from different garnet phlogopite peridotites (Erlank *et al.*, 1987; whole-rock and mineral compositions in Table 3), indicate that the ASU and Alto Paranaíba primary melt compositions can be derived from relatively high melting degrees, i.e. 5–8% of the anhydrous garnet peridotite, or 4–11% of phlogopite-bearing peridotites (Table 3). The presence of a relative K enrichment in the ASU potassic rocks (Fig. 6) suggests that a K-bearing phase (e.g. phlogopite) did not represent a residual phase during partial melting. Phlogopite, instead, was probably a residual phase in the mantle source(s) of the ASU sodic rocks and Alto Paranaíba kamafugites. The primary melts, however, have high abundances of strongly IE and high LREE/HREE ratios, which require mantle sources enriched in IE before or subcontemporaneously with melting process (see Menzies & Wass, 1983). Nd model ages approximately indicate that the IE enrichment in the source mantle of the ASU potassic rocks probably occurred during Middle Proterozoic times (mean 1·5 Ga), whereas those relative to the sodic rocks from eastern Paraguay and Alto Paranaíba kamafugites would be related to Middle–Late Proterozoic events (1·0–0·5 Ga).

Trace element concentrations in the hypothetical mantle sources considered were calculated (batch melting) on the basis of the melting degrees obtained (Table 3) and using the partition coefficients of McKenzie & O'Nions (1991) and Comin-Chiaramonti & Gomes (1996). The multi-elemental plots for the calculated mantle sources, normalized to the primitive mantle of Sun & McDonough (1989), highlight a significant enrichment of the most IE, whereas the least IE (mainly from Zr to Lu) would have concentrations similar to or less than those of primordial mantle (Fig. 9). Notably, the patterns of the mantle sources of the ASU potassic rocks are characterized by negative 'Ta–Nb–Ti' and positive Ba and Sm spikes. On the other hand, the patterns of the mantle sources of both the ASU nephelinites and Alto Paranaíba kamafugites are distinct in their positive Ta–Nb and Zr, and negative K and Sm spikes. It seems, therefore, that the genesis of the ASU alkaline magmatism is dominated by a lithospheric mantle, characterized by small-scale heterogeneity, as also documented by the occurrence of bleb-like glass in spinel peridotite nodules from the ASU nephelinites (Comin-Chiaramonti *et al.*, 1986, 1991). The substantial differences between the mantle source patterns of the ASU potassic rocks and Alto Paranaíba kamafugites (Fig. 9) indicate also a large-scale regional heterogeneity.

The metasomatic processes responsible for mantle incompatible element enrichment are believed to be due mainly to fluids or melts related to subduction processes (e.g. Hergt *et al.*, 1991; Maury *et al.*, 1992) or to volatile-rich small-volume melts from the asthenosphere which would have veined the overlying lithospheric mantle at different depths (e.g. Menzies & Hawkesworth, 1987; Foley, 1992*a*, *b*). In general, the high concentrations of the most IE in all the eastern Paraguay alkaline rocks suggest that the effect of crustal contamination on the Sr–Nd isotope system was negligible and that the parental magma composition was dominated by lithospheric mantle melts.

Depletions in high-field-strength elements, HFSE (Fig. 6), are characteristic of magmatic rocks related to subduction processes, suggesting that mantle IE enrichment may have been caused by fluids or melts derived from a downgoing slab. Following Weaver *et al.* (1987), the ASU potassic rocks with high Ba/Nb and La/Nb ratios could be related to mantle sources contaminated by subducted ocean crust (Ba/Nb = 6·5, La/Nb = 0·7) with the addition of sediments of variable compositions (Ba/Nb = 335–341, La/Nb = 5·7–21·3). Assuming that the mixing processes occurred in the source mantle (2·0–1·4 Ga), ~4–8% of contaminants are required to obtain the Ba/Nb (26–62) and La/Nb (1·6–3·6) ratios of the ASU potassic rocks. The latter process, however, is not supported by geological evidence of a subduction process which would have involved the Rio de La Plata craton in late Early to early Middle Proterozoic times (Bossi *et al.*, 1993). Alternatively, negative HFSE anomalies may result from lithospheric source mantle whose IE enrichment was caused by small-volume melts which left a titanate phase in their solid residua (e.g. Richardson *et al.*, 1982; Haggerty, 1994). It is notable that the ASU sodic rocks, closely associated in space with the potassic analogues, have slightly positive Nb–Ta anomalies (Fig. 6), which indicate that the IE enrichment of the lithospheric source mantle, as proposed for the genesis of the Alto Paranaíba kamafugites by Gibson *et al.* (1995*b*), was produced by low-temperature small-volume asthenospheric melts. This type of enrichment also holds for the sodic magmatism in the Alto Paraguay. The potassic and sodic rocks from eastern Paraguay contain primary carbonates (mean $\delta^{13}C‰$ = 7·04 ± 0·82 VPDB) and are associated with carbonatites

Table 3: Calculated compositions of parental magmas of potassic and sodic rock types from ASU and Alto Paranaíba; compositions of depleted mantle rocks, chemical and mineralogical composition, and mass balances for batch melting of selected mantle rocks

	Calculated parental magmas					Mantle compositions and mineral abundances (wt %)								
	1-B	2-AB	3-Neph	4-Kam		GP	GPP	PP				GP	GPP	PP
SiO_2	47·74	50·40	41·50	40·24	SiO_2	46·24	45·64	45·26			Ol	62·80	65·38	67·45
TiO_2	1·40	1·20	2·55	5·40	TiO_2	0·04	0·06	0·17			Opx	28·35	22·54	20·78
Al_2O_3	10·45	11·01	11·81	5·64	Al_2O_3	1·26	1·40	0·97			Cpx	3·10	5·15	4·56
FeO_t	8·25	8·04	11·11	12·93	FeO_t	6·80	6·81	6·76			Gt	5·75	6·97	
MnO	0·16	0·15	0·23	0·22	MnO	0·12	0·13	0·12			Phl		0·86	7·21
MgO	13·31	12·67	14·27	18·29	MgO	44·31	44·15	44·81			ΣR^2	0·45	0·45	0·72
CaO	11·98	11·08	11·97	13·29	CaO	1·01	1·42	0·86						
Na_2O	2·82	2·14	4·49	0·86	Na_2O	0·09	0·17	0·14						
K_2O	3·42	2·95	0·89	1·83	K_2O	0·09	0·17	0·85						
P_2O_5	0·47	0·36	1·18	1·30	P_2O_5	0·04	0·05	0·06						
mg-no.	0·74	0·74	0·70	0·72	*mg*-no.	0·92	0·92	0·92						
Cr	801	674	545	918										
Ni	710	323	993	749		Mineral mantle compositions								
Rb	45	61	52	189		Ol	Opx	Cpx	Gt	Phl				
Ba	899	1147	1227	10298										
Th	7·5	7·9	9	27·0	SiO_2	41·21	56·70	56·27	43·72	43·96				
U	1·9	2·5	2	7·02	TiO_2	0·05	0·05	0·35	0·05	0·60				
Ta	2·4	2·6	6·7	244	Al_2O_3	0·05	0·91	0·41	20·80	14·81				
Nb	29	23	119	151	FeO_t	7·14	4·47	2·32	7·18	3·31				
La	56	53	126	260	MnO	0·10	0·14		0·49					
Ce	106	103	182	479	MgO	51·58	36·40	17·58	21·33	26·73				
Sr	1124	1038	1215	2734	CaO	0·05	0·34	20·64	6·43					
Nd	48	46	52	209	Na_2O	0·05	0·05	1·81	0·05	0·51				
Sm	12·3	11·3	10·5	28·70	K_2O					10·08				
Zr	121	168	292	772	*mg*-no.	0·93	0·93	0·93	0·84	0·93				
Tb	0·64	0·58	0·71	2·22										
Y	15	16	26	32·6										
Yb	1·4	0·9	1·71	2·22										
Lu	0·21	0·16	0·25	0·24										

	GP				GPP				PP			
SR	1-B	2-AB	3-Neph	4-Kam	1-B	2-AB	3-Neph	4-Kam	1-B	2-AB	3-Neph	4-Kam
Ol	67·8	69·9	65·52	63·7	72·8	75·8	68·54	66·5	73·2	74·3	69·53	68·8
Opx	30·6	29·3	32·76	32·8	26·2	24·2	27·19	27·2	24·3	22·8	24·61	26·5
Cpx	0·0	0·0	0·25	0·3	0·0	0·0	2·07	1·9	0·0	0·3	1·63	0·2
Gt	1·6	0·8	1·47	3·5	1·0	0·0	2·10	4·3	—	—	—	—
Phl	—	—	—	—	0·0	0·0	0·09	0·1	2·5	2·6	4·24	4·53
ΣR^2	0·17	0·14	0·15	0·12	0·12	0·09	0·11	0·10	0·35	0·39	0·44	0·22
F (%)	6·49	7·57	5·66	4·72	9·38	10·72	6·11	4·94	6·98	7·04	4·11	5·43

Calculated parental magmas: 1-B, ASU K basanite [B: Table 2 + 8·9% Ol(Fo_{90}) + 14·8% Cpx($Wo_{46}En_{48}$)]; 2-AB, ASU K alkali basalt [AB: Table 2 + 6·8% Ol(Fo_{90}) + 14·7% Cpx($Wo_{46}En_{48}$)]; 3-Neph, ASU Na nephelinite [Comin-Chiaramonti *et al.* (1991), Table 4, No.1 + 5% Ol(Fo_{93})]; 4-Kam, APIP kamafugite [average of 24 kamafugitic rock-types from Gibson *et al.* (1995*a*), +5% Ol(Fo_{93})]. Mineral–liquid partition coefficients from Caroff *et al.* (1993); *mg*-no. = Mg/(Mg + Fe_{tot}).
Mantle compositions: GP, garnet peridotite [Erlank *et al.* (1987), *n* = 24]; GPP, garnet phlogopite peridotite [Erlank *et al.* (1987), *n* = 24]; PP, phlogopite peridotite [Erlank *et al.* (1987), *n* = 17]. Mantle mineral compositions: Ol, olivine, Opx, orthopyroxene, and Gt, garnet (Nixon, 1987); Cpx, clinopyroxene, and Phl, phlogopite (Erlank *et al.*, 1987).
SR, solid residuum; ΣR^2, sum of the squares of major element residuals; *F* (%), melting degree (see text).

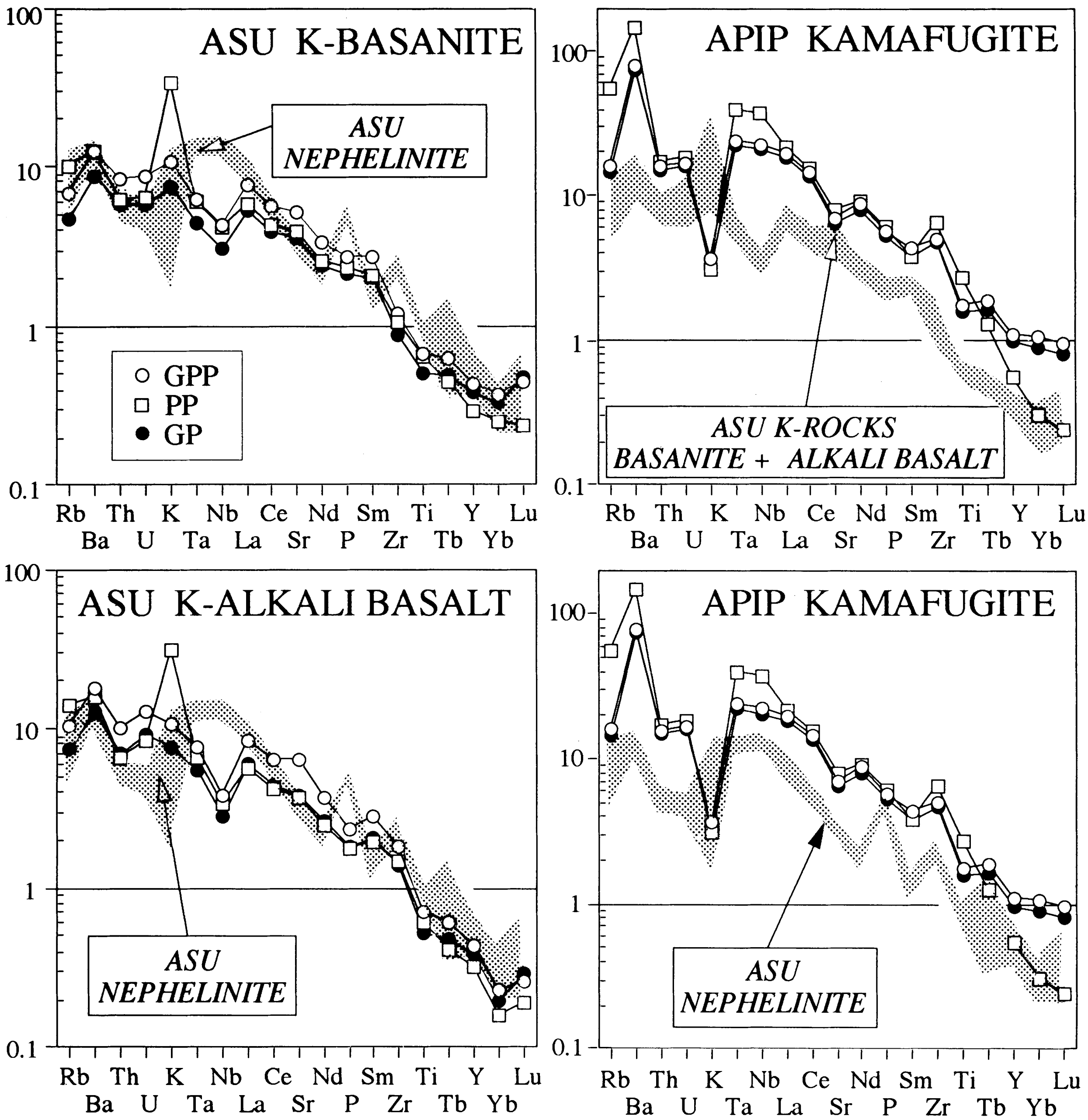

Fig. 9. Calculated concentrations of incompatible elements normalized to primitive mantle (Sun & McDonough, 1989) in the mantle source of eastern Paraguay (ASU) and Alto Paranaíba (APIP), in equilibrium with calculated parental liquids, i.e. basanite 1-B, alkali basalt 2-AB, nephelinite 3-Neph and kamafugite 4-Kam of Table 3, respectively (see text).

whose age ranges from 137 to 128 Ma (Comin-Chiaramonti *et al.*, 1991, 1995). These rocks have Sr and Nd isotope ratios (i.e. $Sr_i = 0{\cdot}70723$–$0{\cdot}70784$ and $Nd_i = 0{\cdot}51136$–$0{\cdot}51183$) similar to those of the ASU potassic rocks. Therefore CO_2 may have played a role in the IE enrichment of the lithospheric mantle, as the volatile-rich fluid–melt compositions are dependent on the CO_2/H_2O ratio (e.g. Dautria *et al.*, 1992; Rudnik *et al.*, 1993).

SIGNIFICANCE OF THE ASU PROVINCE

Crucial to ASU magma genesis is the link with the geodynamic processes which led to the opening of the South Atlantic. According to Nürnberg & Müller (1991) the sea-floor spreading in the South Atlantic at Paraná Basin latitude was initiated at ~125–127 Ma (Chron M4). North of the Walvis–Rio Grande ridges (latitude <28°S) the onset of oceanic crust would be younger (~113 Ma; Chang *et al.*, 1988). In general, the potassic magmatism of the ASU Province is subcoeval with the flood tholeiites of the Paraná Basin and, therefore, occurred during the early stages of rifting, before continental separation. The scarce sodic magmatism, instead, approaches the time of sea-floor spreading (San Juan Bautista, 120 Ma) or corresponds to an advanced stage of continental separation (Asunción, 70–32 Ma). The time of the most significant cooling event in the ASU igneous activity occurred in the Late Cretaceous (80–90 Ma) and overprinted an older thermal perturbation, probably of Early Cretaceous age (Hegarty *et al.*, 1996).

As previously outlined, the alkaline magmatism of eastern Paraguay appears to have derived from a lithospheric source, probably formed by phlogopite-bearing garnet peridotites. Also, the alkaline magmatism of eastern Paraguay and SE Brazil (Morbidelli *et al.*, 1995), as well as that of the Paraná flood tholeiites, was not associated with important lithospheric extension (Piccirillo & Melfi, 1988; Hawkesworth *et al.*, 1992; Turner *et al.*, 1994; Turner & Hawkesworth, 1995; Peate & Hawkesworth, 1996). Therefore, we support the view that the melting process was mainly due to heat released by anomalously hot mantle, i.e. asthenospheric.

The IE enrichment of the source mantle for the alkaline magmatism of eastern Paraguay and SE Brazil occurred in Proterozoic times, 2·0–1·4 and 1·0–0·5 Ga. This enrichment would be related to very small degrees of peridotite melting (e.g. GP in Table 3), possibly ~0·2% (McKenzie, 1989), to match the Sr–Nd isotope ratios of the ASU K rocks.

The alkaline magmatism of Early Cretaceous age may be related to a Mesozoic mantle plume (e.g. Tristan da Cunha?; White & McKenzie, 1989; Richards *et al.*, 1989; Milner & Le Roex, 1996). The heat released from the plume would have partially melted the overlying lithospheric mantle without appreciable contribution from the Mesozoic plume components. It is then suggested that the peripheral distribution of the alkaline magmatism with respect to the Paraná Basin was associated with the cooler margins of the plume system, whereas the subcoeval SGF tholeiites reflect a higher thermal regime, corresponding to the inner and hotter plume regions. It should be noted that the Early Cretaceous alkaline magmatism is volumetrically minor, relative to the Late Cretaceous analogue, and is concentrated in the central area of the Paraná Basin, i.e. eastern Paraguay, the Ponta Grossa Arch and also the Moçamedes arch of Angola (Piccirillo *et al.*, 1990). This contrasts with the alkaline magmatism of Late Cretaceous age, which is voluminous and mostly concentrated in northern Paraná.

According to Gibson *et al.* (1995*b*), the Alto Paranaíba alkaline magmatism of Late Cretaceous age is related to lithospheric mantle source(s) enriched by small-volume melts since Late Proterozoic. Mantle melting would have occurred ~85 Ma ago by heat from a 1000 km wide plume 'head', at present under Trindade. This plume model does not include most alkaline rocks from Serra do Mar, Ponta Grossa–Ipanema and Lages, where several occurrences are subcoeval with those from Alto Paranaíba (e.g. Barra do Teixeira, Cananeia, Tunas; Buzios, Monte de Trigo, São Sebastião and Vitoria islands, Ponta Nova; Morbidelli *et al.*, 1995).

Even assuming that the Trindade plume was smaller and cooler than the Tristan da Cunha plume (~2000 km wide), it seems reasonable to expect that an appreciable volume of tholeiitic basalts, associated with alkaline rocks, would be generated in the inner and hotter (e.g. ~1380°C) portions of the Trindade plume. However, Late Cretaceous tholeiitic basalts are virtually absent, lithospheric extension was very small (β~1·05–1·1; Chang *et al.*, 1992; Ussami *et al.*, 1994) and lithospheric thickness is considerable (>130 km; James *et al.*, 1993). Therefore, we favour a hydrous mantle source or sources at about normal mantle potential temperature (e.g. 1280°C) to generate a relatively small fraction of melt thickness (0·6 km for a mechanical boundary layer 150 km thick; Gallagher & Hawkesworth, 1994), solely from a lithospheric mantle. As the Paraná magmatism probably migrated toward the east and north (Ernesto *et al.*, 1990; Raposo & Ernesto, 1995; Renne *et al.*, 1996*b*), and not from NW to SE (Turner *et al.*, 1994), as recently discussed by Renne *et al.* (1996*a*), we suggest that the Late Cretaceous alkaline magmatism may be related to the anomalous thermal regime responsible for the Paraná tholeiites. The alkaline provinces, developed from the cooler margins of that thermal peak, are thought of as derivative from relatively low melting degrees of lithospheric mantle. It should be noted that over 20–40 Ma were estimated to be required to achieve, from the lithospheric mantle only, ~30–50% of the total melt production with a steady-state potential temperature lower than 1480°C (Hawkesworth *et al.*, 1992). We also suggest that the concentration of the Paraná Late Cretaceous alkaline magmatism along the margin of the São Francisco craton, Ponta Grossa arch and the Serra do Mar probably reflects, at least in part, a tectonic control of the basement (see Santero *et al.*, 1988).

GENETIC RELATIONSHIPS BETWEEN THE ALKALINE AND THOLEIITIC MAGMATISM OF THE PARANÁ BASIN

The geochemical provinciality of the Gondwana flood basalts (low- and high-Ti types; Bellieni *et al.*, 1984*b*; Cox, 1988) is believed to be related to: (1) variable partial melting of an uprising mantle plume (e.g. Campbell & Griffiths, 1990; Arndt *et al.*, 1993) or lithospheric mantle with a variable asthenospheric component (e.g. Piccirillo *et al.*, 1989; Hawkesworth *et al.*, 1992; Peate & Hawkesworth, 1996), followed by variable degrees of crustal contamination (Petrini *et al.*, 1987; Hawkesworth *et al.*, 1988); (2) dehydration melting of heterogeneous subcontinental lithospheric mantle (SCLM), caused by heat released from an underlying mantle plume (Gallagher & Hawkesworth, 1992, 1994); (3) mixing of plume-derived picritic melts with high-potassic melts of lamproitic composition (i.e. high-Ti; Ellam & Cox, 1991); (4) mixing of MORB-like tholeiitic picrites from a mantle plume with high- and low-Ti potassic melts derived from SCLM, followed by crustal contamination (Gibson *et al.*, 1995*a*).

The above hypotheses require an end-member low in IE and with a high Sm/Nd ratio, similar in composition to N-MORB (e.g. Sun & McDonough, 1989). Appropriate end-members with high IE contents, variable IE ratios and low Sm/Nd are required to derive the low- and high-Ti Paraná tholeiites from southern and northern provinces, respectively, by mixing processes. Following Hawkesworth *et al.* (1992), the major difficulty is to explain the genesis of the low-Ti tholeiites, owing to the absence of an end-member with low Ti content, low $^{143}Nd/^{144}Nd$ and high $^{87}Sr/^{86}Sr$ ratios. Castorina *et al.* (1994) demonstrated that this end-member may be represented by the ASU low-Ti potassic mafic rocks (K-ASU; Castorina *et al.*, 1994).

Sr–Nd isotopes

Sr and Nd isotope data indicate that the scarce high-Ti tholeiites from southern Paraná may have originated from SCLM without appreciable N-MORB contribution (Fig. 10a). On the other hand, the dominant H-Ti tholeiites from central and northern Paraná plot on the K-ASU (low-Ti)–N-MORB mixing trend, implying ~20–25% of the K-ASU lithospheric mantle component. The latter isotopic model, however, is not supported by major and trace element data of the low- and high-Ti tholeiites (Piccirillo & Melfi, 1988).

The low-Ti tholeiites from central and northern Paraná conform to the K-ASU–N-MORB mixing curve (Fig. 10b), indicating ~8% (Paraná tholeiites 3064 and 448) to 35% low-Ti mafic potassic melts derived from SCLM as a possible component. The low-Ti tholeiites from southern and a few occurrences from central Paraná trend to higher Sr_i, and are broadly compatible with low-pressure crustal contamination (e.g. AFC; DePaolo, 1981), starting from chemically variable parental melts with positive ε_{Nd} and negative ε_{Sr} (Petrini *et al.*, 1987; Piccirillo *et al.*, 1989). Peate & Hawkesworth (1996) considered the southern Paraná low-Ti 'Gramado-type' magma (i.e. $Sr_i = 0{\cdot}708$–$0{\cdot}710$ and $\varepsilon_{Nd} \sim -3$) as a derivative from a regionally heterogeneous SCLM and interpreted the southern Paraná low-Ti 'Esmeralda-type' magma as the result of mixing between a MORB-like asthenospheric melt (e.g. $\varepsilon_{Nd} = +4$ to $+8$) and a 'Gramado-type' magma.

Assuming that the low-Ti K-ASU and high-Ti Alto Paranaíba kamafugites are derivative from a lithospheric mantle, the expected Sr_i and Nd_i for the Paraná tholeiites would be in the mean ranges 0·7070 (low-Ti) and 0·7050 (high-Ti), and 0·51175 (low-Ti) and 0·51225 (high-Ti), respectively. Therefore, we suggest that the high Sr (and low Nd) isotopic compositions of the Paraná 'Gramado-type' magma reflect a contribution from crustal contamination. Likewise, the 'Esmeralda-type' magma, which reflects a significant N-MORB component (see Paraná tholeiites 3064 and 448, N-MORB; Fig. 10b), was probably contaminated by crustal materials, but to a lesser extent compared with the 'Gramado-type' magma.

Ti–Y–Zr relationships

Ti/Y and Ti/Zr ratios (Fig. 11) show that all the high-Ti Paraná tholeiites are consistent with mixing of a component represented by the Paraná samples 3064 plus 448 and ~15–20% of a high-Ti APIP component. It should be noted that the alkaline lavas from Gough island and Tristan da Cunha (Weaver *et al.*, 1987) would require ~50 and 40% of the latter component, respectively.

The low-Ti tholeiites from central and southern Paraná do not appear to fit the mixing curve N-MORB (or samples 3064 plus 448)–K-ASU, owing to their lower Ti/Y ratios (Fig. 11). The 'Esmeralda-type' and 'Gramado-type' magmas require ~15–25% and up to 40%, respectively, of a siliceous contaminant, similar to the associated Palmas rhyolites (Bellieni *et al.*, 1986; Hawkesworth *et al.*, 1992), or comparable fractions of a mean crystalline basement composition (Piccirillo & Melfi, 1988). Addition of ~4–8% crustal materials (Taylor & McLennan, 1985) to an N-MORB-type source does not account for the low-Ti basalt compositions (see Hergt *et al.*, 1991).

Sr–Nd isotope data show that the high-Ti Paraná tholeiites are not consistent with a mixing curve involving the high-Ti APIP component, a few occurrences from

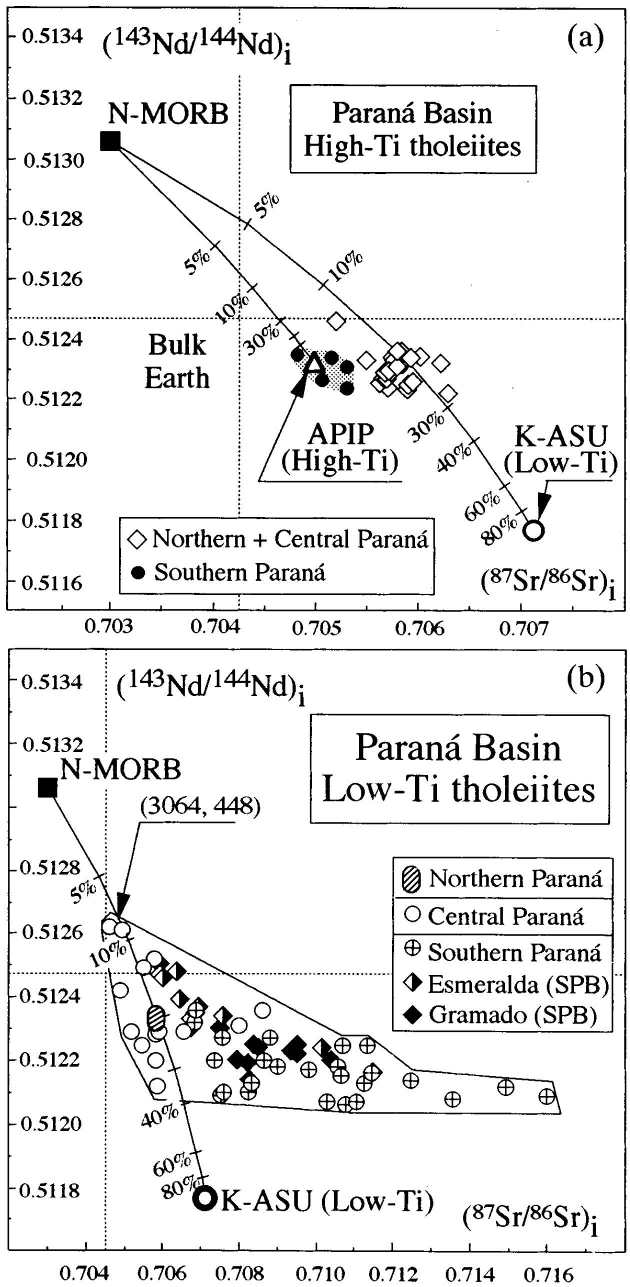

Fig. 10. Comparison of the initial Sr and Nd isotopic ratios of Early Cretaceous flood basalts from the Paraná Basin with average Early Cretaceous (ASU) and late Cretaceous (APIP) mafic potassic rocks from the Paraná Basin. Data sources: APIP, Gibson *et al.* (1995*b*); ASU, Table 1, Comin-Chiaramonti *et al.* (1991, 1992), Comin-Chiaramonti & Gomes (1996); Paraná flood tholeiites and Lages alkaline rock-types: Piccirillo & Melfi (1988); Piccirillo *et al.* (1990); Comin-Chiaramonti *et al.* (1995); Peate & Hawkesworth (1996); Traversa *et al.* (1996); F. Castorina (unpublished data). The mixing curves between N-MORB and average APIP and ASU are also shown. SPB, southern Paraná Basin. Samples 3064 and 448 correspond to southern Paraná low-Ti tholeiites with the highest $^{143}Nd/^{144}Nd$ ratios and flat REE profiles (Marques *et al.*, 1989). (For 'Esmeralda' and 'Gramado' magma types, see text.)

southern Paraná excepted. Notably, the high-Ti Paraná tholeiites do not show evidence of crustal contamination (Petrini *et al.*, 1987; Piccirillo *et al.*, 1989). The Ti/Zr and Ti/Y relationships, instead, indicate that all the high-Ti Paraná tholeiites are compatible with ~15–20% of the APIP-type component. These contrasting results

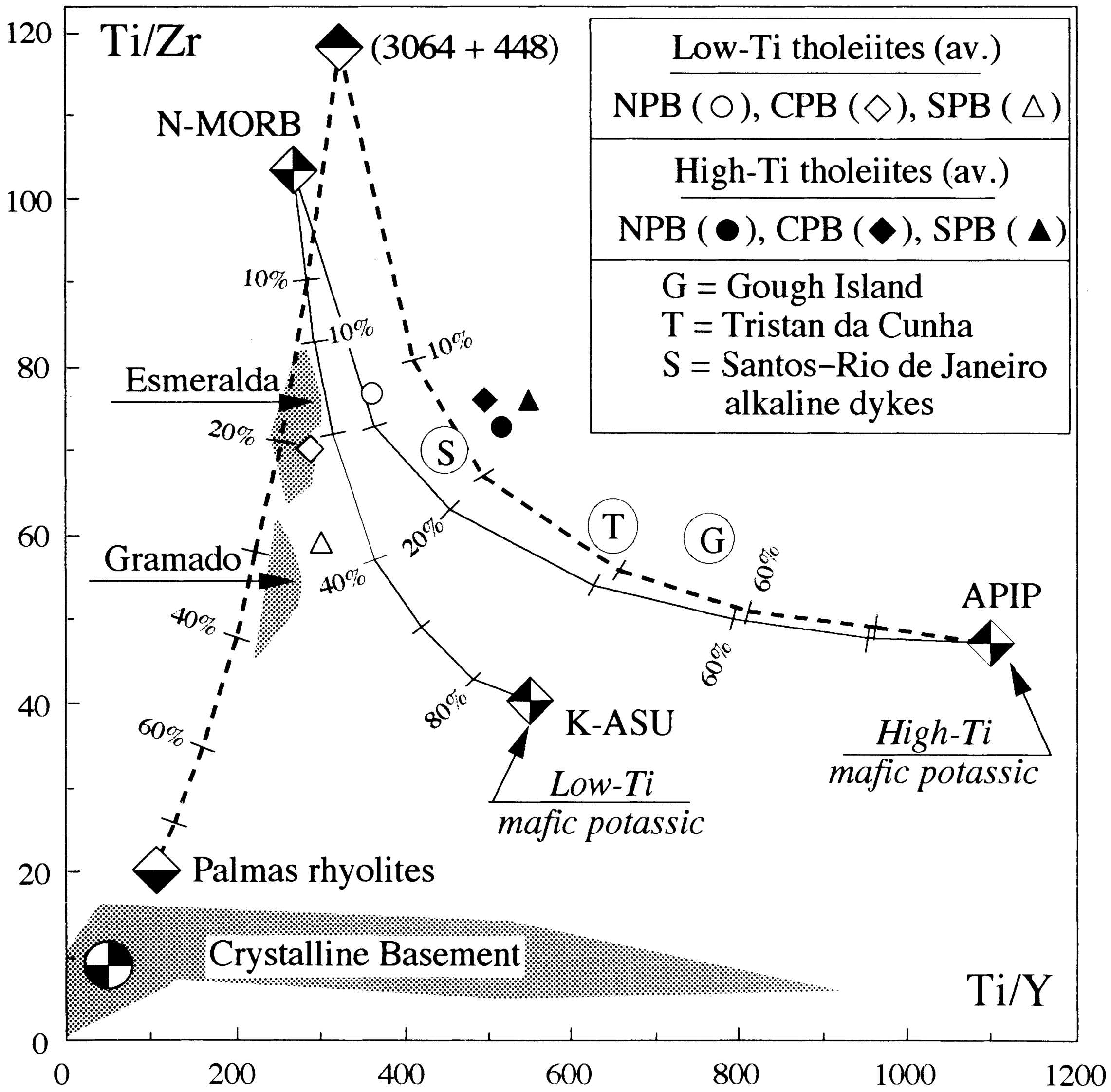

Fig. 11. Zr/Y vs Ti/Y relative to magmatic rock-types from Paraná Basin. Data source, as in Fig. 10; crystalline basement, Piccirillo & Melfi (1988); Gough and Tristan da Cunha, Weaver *et al.* (1987). NPB, CPB, SPB—Northern, Central and Southern Paraná Basin, respectively. (For samples 3064 and 448, see Fig. 10 caption.)

are due, at least partly, to different Nd model ages for Alto Paranaíba kamafugites (818 Ma; Gibson *et al.*, 1995*a*, *b*) and high-Ti Paraná tholeiites (1101 ± 114 Ma), illustrated in Fig. 12. An age difference of 300 Ma would increase Sr_i (130 Ma) of Alto Paranaíba kamafugites from 0·7052 to 0·7059, which fits well the mean value for the Paraná high-Ti basalts, i.e. 0·7058 (Cordani *et al.*, 1988). The Low-Ti Paraná tholeiites, straddling the Sr–Nd isotope mixing curve, indicate 8–35% of low-Ti K-ASU component. The other low-Ti basalts show Sr–Nd isotopes, and Ti/Zr–Ti/Y relationships consistent with crustal contamination which probably occurred during their ascent to the surface.

Metasomatic events

T_{DM} (Nd) model ages (Fig. 12) show that most alkaline rocks, carbonatites and nephelinites from SE Brazil and Paraguay range from 0·5 to 1·1 Ga. This range is virtually the same as that for high-Ti Paraná tholeiites. On the other hand, only K-ASU and carbonatites from eastern

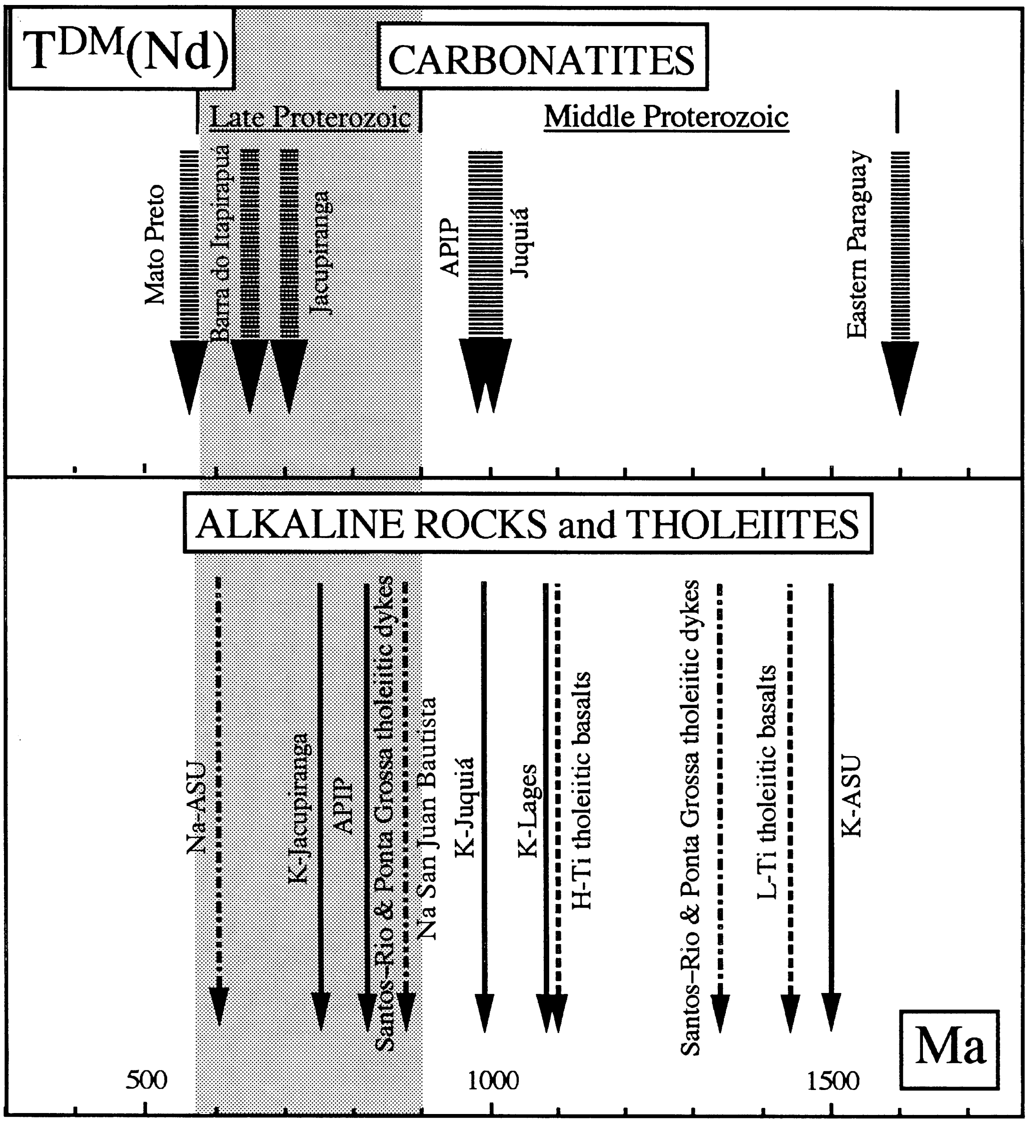

Fig. 12. Mean model ages of igneous rocks from the Paraná Basin. ASU, Asunción; APIP, Alto Paranaíba. Na and K, sodic and potassic rock types, respectively. Data source, as in Fig. 10, and Huang *et al.* (1995).

Paraguay yielded T_{DM} of early Middle Proterozoic age, as did most of the low-Ti Paraná tholeiites, including Santos–Rio de Janeiro and Ponta Grossa tholeiitic dykes.

These model ages indicate that two distinct mantle metasomatic events may have occurred during Middle and Late Proterozoic as precursor to the genesis of tholeiitic and alkaline magmatism in the Paraná Basin. These metasomatic processes were chemically distinct, as indicated by the strong differences in Ti, LILE and HFSE concentrations found in the alkaline rocks (e.g. low-Ti K-ASU vs high-Ti APIP) and tholeiites (low-Ti vs high-Ti types) of the Paraná Basin. The scarce high-Ti tholeiites from southern Paraná actually straddle the boundary between the southern and central regions, and suggest a lithospheric component of APIP type related to metasomatic events of late Middle to early Late Proterozoic times.

In summary, the relationships between the Paraná alkaline and tholeiitic magmatism support a lithospheric mantle origin. Isotopic and IE data indicate that a significant role in the genesis of the Paraná tholeiites was played by an IE-depleted component. The Sr and Nd isotopes (0·7052 and 0·5125, respectively) and other geochemical features of the modern Tristan da Cunha plume (Weaver *et al.*, 1987; Le Roex *et al.*, 1990) are distinctly different from the N-MORB component, and a contribution from the latter is not apparent in the composition of the Paraná tholeiites (Peate & Hawkesworth, 1996). Only some Early Cretaceous tholeiitic basalts ('Tafelkop type') and alkaline rocks ('Okenyenya igneous complex') from Namibia have Sr–Pb isotopes similar to those of Tristan da Cunha, Gough island and Inaccessible Island (Milner & Le Roex, 1996). We support the view that the IE-depleted component is represented by the depleted fractions of a metasomatized, i.e. veined-type mantle. Gibson *et al.* (1995*a*) have suggested that the Paraná flood basalts are the result of a mixing process involving asthenospheric tholeiitic melts, derived from IE-depleted mantle (i.e. Tristan da Cunha plume), and lithospheric K-magmas and that such tholeiites 'may contain up to 50% of mafic potassic lithosphere-derived melts'. This model implies the production (and complete mixing) of an unusually very large volume of alkaline magmas (conservatively, >150 000 km^3) of Early Cretaceous age, which actually are very poorly represented in the entire Paraná Basin.

CONCLUSIONS

(1) Distinct magmatic events are dominant in central–eastern and southwestern Paraguay, i.e. widespread Early Cretaceous potassic magmatism and flood tholeiites (Asunción–Sapucai graben), and sodic magmatism, mainly of Tertiary age (Asunción).

(2) The potassic rocks form a compositional continuum from moderately to strongly potassic. Two suites are proposed, i.e. basanite to phonolite and alkali basalt to trachyte. The sodic rocks include mainly ankaratrites, nephelinites and phonolites.

(3) Two similar but distinct parental magmas emerge for the potassic suites, both characterized by strongly fractionated REE and negative 'Ta–Nb–Ti anomalies'. A slight positive anomaly for Ta and Nb was observed in the sodic rock compositions.

(4) Model crystal fractionation under a low-pressure volcanic regime shows that substantial evolution of the ASU suites may have developed from distinct parental liquids.

(5) Sr–Nd isotope data confirmed the distinction of the potassic rocks, enriched in radiogenic Sr and low in radiogenic Nd, from the sodic rocks, close to BE and transitional to the Paraná flood tholeiites. Crustal contamination does not appear to have been significant in the generation of the investigated rocks. $\delta^{18}O$ data support this conclusion.

(6) The source of potassic rocks is constrained by high LILE, LREE, Th, U and K, relative to a primitive mantle composition.

(7) The close association of potassic and sodic rock suites in the Asunción–Sapucai graben demands that their parental magmas derived from a small subcontinental mantle mass, vertically and laterally heterogeneous in composition and variously enriched in incompatible elements. Significant H_2O, CO_2 and F are also expected in the mantle source from the occurrence of related carbonatites.

(8) Any hypothesis of mantle plume activity at the margin of the Paraná Basin is constrained by distinct lithospheric mantle characteristics. This does not preclude that thermal perturbations from the asthenosphere may have triggered magmatic activity in the lithospheric mantle in eastern Paraguay.

(9) It is proposed that an isotopically enriched source, implied by the ASU potassic magmas, derived from a depleted lithospheric mantle pervasively invaded by IE–C–H-rich fluids. These are expected to have promoted crystallization of K-rich phases (e.g. phlogopite) in a pristine peridotite, where they developed a veined network variously enriched in LILE and LREE under various redox conditions. The newly formed veins ('enriched component') and peridotite matrix ('depleted component') underwent a different isotopic evolution with time, depending on their parent/daughter ratio. This model was extended to the Paraná flood tholeiites and to high- and low-Ti potassic magmatism from southeastern Brazil.

(10) Isotopically distinct magmas were generated following two 'enrichment' events of the subcontinental upper mantle estimated at 2·0–1·4 Ma and 1·0–0·5 Ga, respectively. This would have preserved isotopic heterogeneities over a long period of time, pointing to a non-convective lithospheric mantle beneath different cratons or intercratonic regions.

(11) The occurrence of potassic magmatism in the Paraná Basin implies appropriate lithospheric sources to generate also the flood tholeiites. Therefore, the hypothesis of an asthenospheric plume origin is not compelling other than as a thermal perturbation and a possible source for the Mesozoic plume melts which contaminated the lithosphere.

ACKNOWLEDGEMENTS

We are grateful to S. Milner, S. Turner and particularly to A. Ewart for their careful and constructive reviews of an earlier version of the manuscript. We also offer our thanks to R. Alaimo for the use of ICP-MS at CEPA Institution (Palermo). A. C. thanks the Staff of GEOTRACK International at the University of Melbourne for their hospitality and assistance during the preparation of this paper. Financial support from Italian (CNR and MURST) and Brazilian (FAPESP) agencies is gratefully acknowledged.

REFERENCES

Alaimo, R. & Censi, P., 1992. Quantitative determination of major, minor and trace elements on U.S.G.S. rock standards by inductively coupled plasma mass spectrometry. *Atomic Spectrometry* **13,** 113–119.

Arndt, N. T., Czamanske, G. K., Wooden, J. L. & Federenko, V. A., 1993. Mantle and crustal contributions to continental flood volcanism. *Tectonophysics* **223,** 39–52.

Barton, M., 1979. A comparative study of some minerals occurring in the K-rich alkaline rocks of the Leucite Hills, Wyoming, the Vico vulcano, Italy, and the Toro-Ankole region, Uganda. *Neues Jahrbuch für Mineralogie, Abhandlungen* **137,** 113–134.

Beccaluva, L., Di Girolamo, P. & Serri, G., 1991. Petrogenesis and tectonic setting of the Roman Volcanic Province, Italy. *Lithos* **26,** 191–221.

Bellieni, G., Brotzu, P., Comin-Chiaramonti, P., Ernesto, M., , Melfi, A. J., Pacca, I. G., Piccirillo, E. M. & Stolfa, D., 1984*a*. Flood basalt to rhyolite suites in the southern Paraná plateau (Brazil): paleomagnetism, petrogenesis and geodynamic implications. *Journal of Petrology* **25,** 579–618.

Bellieni, G., Comin-Chiaramonti, P., Marques, L. S., Melfi, A. J., Nardy, A. J. R., Piccirillo, E. M., Stolfa, D. & Roisemberg, A., 1984*b*. High- and low-TiO_2 flood basalts from the Paraná plateau (Brazil): petrology and geochemical aspects bearing on their mantle origin. *Neues Jahrbuch für Mineralogie, Abhandlungen* **150,** 273–306.

Bellieni, G., Comin-Chiaramonti, P., Marques, L. S., Melfi, A. J., Nardy, A. J. R., Papatrechas, C., Piccirillo, E. M. & Stolfa, D., 1986. Petrogenetic aspects of acid and basaltic lavas from the Paraná plateau (Brazil): geological, mineralogical and petrochemical relationships. *Journal of Petrology* **27,** 844–915.

Bergman, S. C., 1987. Lamproites and other potassium-rich igneous rocks: a review of their occurrence, mineralogy and geochemistry. In: Fitton, J. G. & Upton, B. G. J. (eds) *Alkaline Igneous Rocks. Special Publication, Geological Society of London* **30,** 103–190.

Bossi, J., Campal, N., Civetta, L., Demarchi, G., Girardi, V., Mazzucchelli, M., Negrini, L., Rivalenti, G., Fragoso Cesar, A. R. S., Sinigoi, S., Teixeira, W., Piccirillo, E. M. & Molesini, M., 1993. Early Proterozoic dyke swarm from western Uruguay: geochemistry, Sr–Nd isotopes and petrogenesis. *Chemical Geology* **106,** 263–277.

Boynton, W. V., 1984. Cosmochemistry of the rare earth elements: meteorite studies. In: Henderson, P. (ed.) *Rare Earth Element Geochemistry*. Amsterdam: Elsevier, pp. 63–114.

Campbell, I. H. & Griffiths, R. W., 1990. Implications of mantle plume structure for the evolution of flood basalts. *Earth and Planetary Science Letters* **99**, 79–93.

Caroff, M., Maury, R. C., Leterrier, J., Joron, J. L., Cotten, J. & Guille, G., 1993. Trace element behaviour in the alkali basalt–comenditic trachyte series from Mururoa Atoll, French Polynesia. *Lithos* **30,** 1–22.

Castorina, F., Censi, P., Barbieri, M., Comin-Chiaramonti, P., Cundari, A. & Gomes, C. B., 1994. Carbonatites from the Paraná basin: a 130 Ma transect. In: *International Symposium on the Physics and Chemistry of the Upper Mantle, São Paulo, Brazil.* Extended Abstract, pp. 52–55.

Chang, H. K., Kowsmann, R. O. & de Figuereido, M. F., 1988. New concept on the development of east Brazilian marginal basins. *Episodes* **11,** 194–202.

Chang, H. K., Kowsmann, R. O., Figuereido, A. M. F. & Bender, A. A., 1992. Tectonics and stratigraphy of the East Brazil Rift System. *Tectonophysics* **213,** 97–138.

Comin-Chiaramonti, P. & Gomes, C. B., 1996. *Alkaline Magmatism in Central–Eastern Paraguay. Relationships with Coeval Magmatism in Brazil.* São Paulo: Edusp–Fapesp, 432 pp.

Comin-Chiaramonti, P., Demarchi, G., Girardi, V. A. V., Princivalle, F. & Sinigoi, S., 1986. Evidence of mantle metasomatism and heterogeneity from peridotite inclusions of northeastern Brazil and Paraguay. *Earth and Planetary Science Letters* **77,** 203–217.

Comin-Chiaramonti, P., Civetta, L., Petrini, R., Piccirillo, E. M., Bellieni, G., Censi, P., Bitschene, P., Demarchi, G., De Min, A., Gomes, C. B., Castillo, A. M. C. & Velazquez, J. C., 1991. Tertiary nephelinitic magmatism in Eastern Paraguay: petrology, Sr–Nd isotopes and genetic relationships with associated spinel-peridotite xenoliths. *European Journal of Mineralogy* **3,** 507–525.

Comin-Chiaramonti, P., Cundari, A., Gomes, C. B., Piccirillo, E. M., Censi, P., De Min, A., Bellieni, G., Velazquez, V. F. & Orué, D., 1992. Potassic dyke swarm in the Sapucai graben, Eastern Paraguay: petrographical, mineralogical and geochemical outlines. *Lithos* **28,** 283–301.

Comin-Chiaramonti, P., Castorina, F., Cundari, A., Petrini, R. & Gomes, C. B., 1995. Dykes and sills from Eastern Paraguay: Sr and Nd isotope systematics. In: Baer, G. & Heimann, A. (eds) *Physics and Chemistry of Dykes*. Rotterdam: Balkema, pp. 267–278.

Cordani, U. G., Civetta, L., Mantovani, M. S. M., Petrini, R., Kawashita, K., Hawkesworth, C. J., Taylor, P., Longinelli, A., Cavazzini, G. & Piccirillo, E. M., 1988. Isotope geochemistry of flood volcanics from the Paraná Basin (Brazil). In: *The Mesozoic Flood Volcanism from the Paraná Basin (Brazil). Petrogenetic and Geophysical Aspects.* São Paulo: Iag-Usp, pp. 157–178.

Cox, K. G., 1988. The Karoo province. In: MacDougall, J. D. (ed.) *Continental Flood Basalts*. Dordrecht: Kluwer Academic, pp. 239–271.

Dautria, J. M., Dupuy, C., Takherist, D. & Dostal, J., 1992. Carbonate metasomatism in the lithospheric mantle: peridotitic xenoliths from a melilitic district of the Sahara Basin. *Contributions to Mineralogy and Petrology* **111,** 37–52.

de la Roche, H., 1986. Classification et nomenclature des roches ignées: un essai de restauration de la convergence entre systématique quantitative, typologie d'usage et modélisation génétique. *Bulletin de la Societé Geologique de France* **8,** 337–353.

DePaolo, D. J., 1981. Trace element and isotopic effects of combined wallrock assimilation and fractional crystallization. *Earth and Planetary Science Letters* **43,** 201–211.

Ellam, R. M. & Cox, K. G., 1991. An interpretation of Karoo picrite basalts in terms of interaction between asthenospheric magmas and mantle lithosphere. *Earth and Planetary Science Letters* **105,** 330–342.

Erlank, A. J., Waters, F. G., Hawkesworth, C. J., Haggerty, S. E., Allsopp, H. L., Rickard, R. S. & Menzies, M. A., 1987. Evidence for mantle metasomatism in peridotite nodules from the Kimberley pipes, South Africa. In: Menzies M. A. & Hawkesworth C. J. (eds) *Mantle Metasomatism*. London: Academic Press, pp. 221–311.

Ernesto, M., Pacca, I. G., Hiodo, F. Y. & Nardy, A. J. R., 1990. Palaeomagnetism of the Mesozoic Serra Geral Formation, southern Brazil. *Physics of the Earth and Planetary Interiors* **64,** 153–175.

Ewart, A., 1989. East Australian petrology and geochemistry. In: Johnson, R.W. (ed.) *Intraplate Volcanism in Eastern Australia and New Zealand*. Cambridge: Cambridge University Press, pp. 189–248.

Ewart, A., Chappell, B. W. & Menzies, M. A., 1988. An overview of the geochemical and isotopic characteristics of the Eastern Australian Cainozoic Volcanic Province. *Journal of Petrology, Special Lithosphere Issue*, pp. 225–273.

Foley, S. F., 1988. The genesis of continental basic alkaline magmas. An interpretation in terms of redox melting. *Journal of Petrology, Special Lithosphere Issue*, pp. 139–161.

Foley, S. F., 1992*a*. Petrological characterization of the source components of potassic magmas: geochemical and experimental constraints. *Lithos* **28,** 187–204.

Foley, S. F., 1992*b*. Vein plus wall-rock melting mechanism in the lithosphere and the origin of potassic alkaline magmas. *Lithos* **28,** 435–453.

Foley, S. F., Venturelli, G., Green, D. H. & Toscani, L., 1987. The ultrapotassic rocks; characteristics, classification and constraints for petrogenetic modes. *Earth-Science Reviews* **24,** 81–134.

Fulfaro, V. J., 1996. Geology of Eastern Paraguay. In: Comin-Chiaramonti, P. & Gomes, C. B. (eds) *Alkaline Magmatism in Central–Eastern Paraguay. Relationships with Coeval Magmatism in Brazil.* São Paulo: Edusp–Fapesp, pp. 1–13.

Gallagher, K. & Hawkesworth, C. J., 1992. Dehydration melting and the generation of continental flood basalts. *Nature* **358,** 57–59.

Gallagher, K. & Hawkesworth, C. J., 1994. Mantle plumes, continental magmatism and asymmetry in the South Atlantic. *Earth and Planetary Science Letters* **123,** 105–117.

Gibson, S. A., Thompson, R. N., Dickin, A. P. & Leonardos, O. H., 1995*a*. High-Ti and low-Ti mafic potassic magmas: key to plume–lithosphere interactions and continental flood-basalt genesis. *Earth and Planetary Science Letters* **136,** 149–165.

Gibson, S. A., Thompson, R. N., Leonardos, O. H., Dickin, A. P. & Mitchell, J. G., 1995*b*. The Late Cretaceous impact of the Trindade mantle plume; evidence from large-volume, mafic, potassic magmatism in SE Brazil. *Journal of Petrology* **36,** 189–229.

Haggerty, S. E., 1994. Upper mantle mineralogy. In: *International Symposium on the Physics and Chemistry of the Upper Mantle*, São Paulo, Invited Lectures, pp. 33–82.

Hart, R. S., Gerlach, D. C. & White, W. M., 1986. A possible Sr–Nd–Pb mantle array and consequences for mantle mixing. *Geochimica et Cosmochimica Acta* **50,** 1551–1557.

Hawkesworth, C. J., Mantovani, M. & Peate, D., 1988. Lithosphere remobilization during Paraná CFB magmatism. *Journal of Petrology, Special Lithosphere Issue*, pp. 205–223.

Hawkesworth, C. J., Gallagher, K., Kelley, S., Mantovani, M., Peate, D. W., Regelous, M. & Rogers, N.W., 1992. Paraná magmatism and the opening of the South Atlantic. In: Storey, B. C., Alabaster, T. & Pankhurst, R. J. (eds) *Magmatism and the Causes of Continental Break-up. Special Publication, Geological Society of London* **68,** 221–240.

Hegarty, K. A., Duddy, I. R. & Green, P. F., 1996. The thermal history in and around the Paraná Basin using apatite track analysis: implications for hydrocarbon occurrences and basin formation. In: Comin-Chiaramonti, P. & Gomes, C. B. (eds) *Alkaline Magmatism in Paraguay and Relationships with Coeval Magmatism in Brazil.* São Paulo: Edusp–Fapesp, pp. 41–50.

Hergt, J. M., Peate, D. W. & Hawkesworth, C. J., 1991. The petrogenesis of Mesozoic Gondwana low-Ti flood basalts. *Earth and Planetary Science Letters* **105,** 134–148.

Huang, H.-M., Hawkesworth, C. J., van Calsteren, P. & McDermott, F., 1995. Geochemical characteristics and origin of the Jacupiranga carbonatites, Brazil. *Chemical Geology* **119,** 79–99.

James, D. E., Assumpção, M., Snoke, J. A., Ribotta, L. C. & Kuehnel, R., 1993. Seismic studies of continental lithosphere beneath SE Brazil. *3rd Congress of the Brazilian Geophysical Society*, Rio de Janeiro, Expanded Abstracts 2, pp. 1110–1115.

LeBas, M. J., LeMaitre, R. W., Streckeisen, A. & Zanettin, B., 1986. A chemical classification of volcanic rock based on the total alkali–silica diagram. *Journal of Petrology* **27,** 745–750.

LeMaitre, R. W., 1989. *A Classification of Igneous Rocks and Glossary of Terms.* Oxford: Blackwell, 193 pp.

Le Roex, A. P., Cliff, R. A. & Adair, B. J. J., 1990. Tristan da Cunha, South Atlantic: geochemistry and petrogenesis of a basanite–phonolite lava series. *Journal of Petrology* **31,** 779–812.

Ludwig, K. R., 1987. User's guide for 'analyst', a computer program for control of an isomass 54e thermal-ionization, single collector mass-spectrometer. *US Geological Survey Open File Report*, pp. 485–513.

Marques, L. S., Piccirillo, E. M., Melfi, A. J., Comin-Chiaramonti, P. & Bellieni, P., 1989. Distribução de terras raras e outros elementos traços em basaltos da Bacia do Paraná (Brasil Meridional). *Geochimica Brasiliensis* **3,** 33–50.

Marzoli, A., 1991. Studio petrologico e geochimico di complessi alcalini del rift di Sapucai (Paraguay). B.Sc. Thesis, Trieste University, 201 pp.

Maury, R., Defant, C. & Joron, M. J., 1992. Metasomatism of the sub-arc mantle inferred from trace elements in Philippine xenoliths. *Nature* **360,** 661.

McKenzie, D. P., 1989. Some remarks on the movement of small melt fractions in the mantle. *Earth and Planetary Science Letters* **95,** 53–72.

McKenzie, D. P. & O'Nions, R. K., 1991. Partial melt distributions from inversion of rare earth element concentrations. *Journal of Petrology* **32,** 1021–1091.

McKenzie, D. P. & O'Nions, M. J., 1995. The source regions of ocean island basalts. *Journal of Petrology* **36,** 133–159.

Menzies, M. A. & Hawkesworth, C. J. (eds), 1987. *Mantle Metasomatism.* London: Academic Press, 472 pp.

Menzies, M. A. & Wass, S. Y., 1983. CO_2 and LREE-rich mantle below eastern Australia; a REE and isotopic study of alkaline magmas and apatite-rich mantle xenoliths from the Southern Highlands Province, Australia. *Earth and Planetary Science Letters* **65,** 287–302.

Milner, S. C. & le Roex, A. P., 1996. Isotope characteristics of the Okenyenya igneous complex, northwestern Namibia: constraints on the composition of the early Tristan plume and the origin of the EM 1 mantle component. *Earth and Planetary Science Letters* **141,** 277–291.

Mitchell, R. H. & Bergman, S. C. (eds), 1991. *Petrology of Lamproites.* New York: Plenum, 447 pp.

Morbidelli, L., Gomes, C. B., Beccaluva, L., Brotzu, P., Conte, A.M., Ruberti, E. & Traversa, G., 1995. Mineralogical, petrological and geochemical aspects of alkaline and alkaline-carbonatite associations from Brazil. *Earth-Science Reviews* **30,** 135–168.

Nixon, P. H. (ed.), 1987. *Mantle Xenoliths.* Chichester: John Wiley, 844 pp.

Nürnberg, D. & Müller, R. D., 1991. The tectonic evolution of the South Atlantic from Late Jurassic to present. *Tectonophysics* **191,** 27–43.

O'Hara, M. J. & Mathews, R. E., 1981. Geochemical evolution of an advancing periodically replenished magma chamber. *Journal of the Geological Society, London* **138,** 237–277.

Pearce, J. A., 1983. Role of the sub-continental lithosphere in magma genesis at active continental margins. In: Hawkesworth, C. J. & Norry, M. J. (eds) *Continental Basalts and Mantle Xenoliths.* Nantwich, UK: Shiva, pp. 230–249.

Peate, D. W. & Hawkesworth, C. J., 1996. Lithospheric to asthenospheric transition in low-Ti flood basalts from Southern Paraná, Brazil. *Chemical Geology* **127,** 1–24.

Petrini, R., Civetta, L., Piccirillo, E. M., Bellieni, G., Comin-Chiaramonti, P., Marques, L. S. & Melfi, A. J., 1987. Mantle heterogeneity and crustal contamination in the genesis of low-Ti continental flood basalts from the Paraná plateau (Brazil): Sr–Nd isotope and geochemical evidence. *Journal of Petrology* **28,** 701–726.

Piccirillo, E. M. & Melfi, A. J. (eds), 1988. *The Mesozoic Flood Volcanism from the Paraná Basin (Brazil). Petrogenetic and Geophysical Aspects.* São Paulo: Iag-Usp, 600 pp.

Piccirillo, E. M., Civetta, L., Petrini, R., Longinelli, A., Bellieni, G., Comin-Chiaramonti, P., Marques, L. S. & Melfi, A. J., 1989. Regional variations within the Paraná flood basalts (Southern Brazil): evidence for subcontinental mantle heterogeneity and crustal contamination. *Chemical Geology* **75,** 103–122.

Piccirillo, E. M., Bellieni, G., Cavazzini, G., Comin-Chiaramonti, P., Petrini, R., Melfi, A. J., Pinese, J. P. P., Zantedeschi, P. & De Min, A., 1990. Lower Cretaceous dyke swarms from the Ponta Grossa arch. Petrology, Sm–Nd isotopes and genetic relationships with the Paraná flood volcanics. *Chemical Geology* **89,** 19–48.

Raposo, M. I. B. & Ernesto, M., 1995. An Early Cretaceous paleomagnetic pole from Ponta Grossa dikes (Brazil): implications for the South American Mesozoic apparent polar wander path. *Journal of Geophysical Research* **100**(B10), 20095–20109.

Renne, P. R., Ernesto, M., Pacca, I. G., Coe, R. S., Glen, J. M., Prévot, M. & Perrin, M., 1992. The age of Paraná flood volcanism, rifting of Gondwanaland, and Jurassic–Cretaceous boundary. *Science* **258,** 975–979.

Renne, P. R., Mertz, D. F., Teixeira, W., Ens, H. & Richards, M., 1993. Geochronologic constraints on magmatic and tectonic evolution of the Paraná Province. *American Geophysical Union Abstract, EOS* **74,** 553.

Renne, P. R., Glen, J. M., Milner, S. C. & Duncan, A. R., 1996*a*. Age of Etendeka flood volcanism and associated intrusions in southwestern Africa. *Geology* **24,** 659–662.

Renne, P. R., Deckart, K., Ernesto, M., Féraud, G. & Piccirillo, E. M., 1996*b*. Age of the Ponta Grossa dike swarm (Brazil), and implications to Paraná flood volcanism. *Earth and Planetary Science Letters* (in press).

Richards, M. A., Duncan, R. A. & Courtillot, V. E., 1989. Floods basalts and hot spot tracks: plume heads and tails. *Science* **246,** 103–107.

Richardson, S. H., Erlank, A. J., Duncan, A. R. & Reid, D. L., 1982. Correlated Sr, Nd and Pb isotope variations in Walvis Ridge basalts and implications for the evolution of their mantle source. *Earth and Planetary Science Letters* **59,** 327–342.

Rudnik, R. L., McDonough, W. F. & Chappell, B. W., 1993. Carbonatite metasomatism in the northern Tanzanian mantle: petrographic and geochemical characteristics. *Earth and Planetary Science Letters* **114,** 463–475.

Santero, P., Zadro, M., Blitzkow, D. & de Sá, N. C., 1988. Gravimetric analysis of the Goiânia flexure, northern Paraná basin. In: Piccirillo, E. M. & Melfi, A. J. (eds) *The Mesozoic Flood Volcanism from the Paraná Basin (Brazil). Petrogenetic and Geophysical Aspects*. São Paulo: Iag-Usp, pp. 257–269.

Streckeisen, A. 1976. To each plutonic rock its proper name. *Earth-Science Reviews* **12,** 1–33.

Sun, S.-S. & McDonough, W. F., 1989. Chemical and isotopic systematics of oceanic basalts: implications for mantle composition and processes. In: Saunders, A. D. & Norry, M. J. (eds) *Magmatism in the Ocean Basins. Special Publication, Geological Society of London* **42,** 313–345.

Taylor, S. R. & McLennan, S. M., 1985. *The Continental Crust; its Composition and Evolution.* Oxford: Blackwell Scientific, 312 pp.

Traversa, G., Barbieri, M., Beccaluva, L., Coltorti, M., Conte, A.M., Garbarino, C., Gomes, C. B., Macciotta, G., Morbidelli, L., Ronca, S. & Scheibe, L. F., 1996. Mantle sources and differentiation of alkaline magmatic suite of Lages, Santa Catarina, Brazil. *European Journal of Mineralogy* **8,** 193–208.

Turner, S. & Hawkesworth, C. J., 1995. The nature of the subcontinental mantle: constraints from the major element composition of continental flood-basalts. *Chemical Geology* **120,** 295–314.

Turner, S., Regelous, M., Kelley, S., Hawkesworth, C. J. & Mantovani, M., 1994. Magmatism and continental break-up in the South Atlantic: high precision ^{40}Ar–^{39}Ar geochronology. *Earth and Planetary Science Letters* **121,** 333–348.

Ussami, N., Kolisnyk, A., Raposo, M. I. B., Ferreira, F. J. F., Molina, E. C. & Ernesto, M., 1994. Detectabilitade magnetica de diques do Arco de Ponta Grossa: um estudo integrado de magnetometria terrestre/aerea e magnetismo de rocha. *Revista Brasileira de Geocências* **21,** 317–327.

Weaver, B. L., Wood, D. A., Tarney, J. & Joron, J. L., 1987. Geochemistry of ocean island basalts from South Atlantic: Ascension, Bouvet, St. Helena, Gough and Tristan da Cunha. In: Fitton, J. G. & Upton, B. G. (eds) *Akaline Igneous Rocks. Special Publication, Geological Society of London* **30,** 253–267.

White, R. S. & McKenzie, D. P., 1989. Magmatism at rift zones. *Journal of Geophysical Research* **94,** 11933–11944.

Wyllie, P. J., 1987. Volcanic rocks: boundaries from experimental petrology. *Fortschrifte für Mineralogie* **65,** 249–284.

Zindler, A. & Hart, S. R., 1986. Chemical geodynamics. *Annual Review of Earth and Planetary Sciences* **14,** 493–571.